

An inter-laboratory comparison of aerosol inorganic ion measurements by Ion Chromatography: implications for aerosol pH estimate

Jingsha Xu¹, Shaojie Song², Roy M. Harrison¹, Congbo Song¹, Lianfang Wei³, Qiang Zhang⁴, Yele Sun³, Lu Lei³, Chao Zhang⁵, Xiaohong Yao^{5, 6}, Dihui Chen⁵, Weijun Li⁷, Miaomiao Wu⁷, Hezhong Tian⁸, Lining Luo⁸, Shengrui Tong⁹, Weiran Li⁹, Junling Wang¹⁰, Guoliang Shi¹¹, Yanqi Huangfu¹¹, Yingze Tian¹¹, Baozhu Ge³, Shaoli Su¹², Chao Peng¹², Yang Chen¹², Fumo Yang¹³, Aleksandra Mihajlidi-Zelić¹⁴, Dragana Đorđević¹⁴, Stefan J. Swift¹⁵, Imogen Andrews¹⁵, Jacqueline F. Hamilton¹⁵, Ye Sun¹⁶, Agung Kramawijaya¹, Jinxiu Han¹, Supattarachai Saksakulkrai¹, Clarissa Baldo¹, Siqi Hou¹, Feixue Zheng¹⁷, Kaspar R. Daellenbach¹⁷, Chao Yan¹⁷, Yongchun Liu¹⁷, Markku Kulmala¹⁷, Pingqing Fu⁴, Zongbo Shi*¹

1 School of Geography Earth and Environmental Science, University of Birmingham, Birmingham, B15 2TT, UK

2 School of Engineering and Applied Sciences, Harvard University, Cambridge, MA 02138, USA

3 State Key Laboratory of Atmospheric Boundary Layer Physics and Atmospheric Chemistry, Institute of Atmospheric Physics, Chinese Academy of Sciences, Beijing, 100029, China

4 Institute of Surface-Earth System Science, Tianjin University, Tianjin, 300072, China

5 Frontiers Science Center for Deep Ocean Multispheres and Earth System, and Key Laboratory of Marine Environment and Ecology, Ministry of Education of China, Ocean University of China, Qingdao 266100, China

6 Laboratory for Marine Ecology and Environmental Sciences, Qingdao National Laboratory for Marine Science and Technology, Qingdao 266071, China

7 Department of Atmospheric Sciences, School of Earth Sciences, Zhejiang University, Hangzhou, 310027, China

8 Center for Atmospheric Environmental Studies, Beijing Normal University, Beijing, 100875, China

9 State Key Laboratory of Structural Chemistry of Unstable and Stable Species, Institute of Chemistry, Chinese Academy of Sciences, Beijing, 100190, China

10 School of Environment, Tsinghua University, Beijing, 100084, China

11 State Environmental Protection Key Laboratory of Urban Ambient Air Particulate Matter Pollution Prevention and Control, Center for Urban Transport Emission Research, College of Environmental Science and Engineering, Nankai University, Tianjin, 300350, China

12 Research Center for Atmospheric Environment, Chongqing Institute of Green and Intelligent Technology, Chinese Academy of Sciences, Chongqing, 400714, China

13 Department of Environmental Science and Engineering, Sichuan University, Chengdu, 610065, China

14 Centre of Excellence in Environmental Chemistry and Engineering – ICTM, University of Belgrade, Njegoševa 12 (Studentski trg 14–16), Belgrade, Serbia

15 Department of Chemistry, University of York, York, YO10 5DD, UK

16 School of Space and Environment, Beihang University, Beijing, 100191, China

17 Beijing Advanced Innovation Center for Soft Matter Science and Engineering, Beijing University of Chemical Technology, Beijing, 100029, China

Correspondence: Zongbo Shi (Z.Shi@bham.ac.uk)

37 **ABSTRACT**

38 Water soluble inorganic ions such as ammonium, nitrate, and sulfate are major components of fine
39 aerosols in the atmosphere and are widely used in the estimation of aerosol acidity. However, different
40 experimental practices and instrumentation may lead to uncertainties in ion concentrations. Here, an
41 inter-comparison experiment was conducted in 10 different laboratories (labs) to investigate the
42 consistency of inorganic ion concentrations and resultant aerosol acidity estimates using the same set
43 of aerosol filter samples. The results mostly exhibited good agreement for major ions Cl^- , SO_4^{2-} , NO_3^- ,
44 NH_4^+ and K^+ . However, F^- , Mg^{2+} and Ca^{2+} were observed with more variations across the different
45 labs. The Aerosol Chemical Speciation Monitor (ACSM) data of non-refractory SO_4^{2-} , NO_3^- , NH_4^+
46 generally correlated very well with the filter analysis based data in our study, but the absolute
47 concentrations differ by up to 42%. Cl^- from the two methods are correlated but the concentration
48 differ by more than a factor of three. The analyses of certified reference materials (CRMs) generally
49 showed good detection accuracy (DA) of all ions in all the labs, the majority of which ranged between
50 90% and 110%. The DA was also used to correct the ion concentrations to showcase the importance
51 of using CRM for calibration check and quality control. Better agreements were found for Cl^- , SO_4^{2-} ,
52 NO_3^- , NH_4^+ and K^+ across the labs after their concentrations were corrected with DA; the coefficient
53 of variation (CV) of Cl^- , SO_4^{2-} , NO_3^- , NH_4^+ and K^+ decreased 1.7%, 3.4%, 3.4%, 1.2% and 2.6%,
54 respectively, after DA correction. We found that the ratio of anion to cation equivalent concentrations
55 (AE/CE) and Ion balance (anions – cations) are not a good indicator for aerosol acidity estimates,
56 as the results in different labs did not agree well with each other. In situ aerosol pH calculated from
57 the ISORROPIA-II thermodynamic equilibrium model with measured ion and ammonia
58 concentrations showed a similar trend and good agreement across the 10 labs. Our results indicate
59 that although there are important uncertainties in aerosol ion concentration measurements, the
60 estimated aerosol pH from the ISORROPIA-II model is more consistent.

61 **Keywords:** $\text{PM}_{2.5}$, inorganic ions, aerosol acidity, ion balance, thermodynamic model

62

63 1. INTRODUCTION

64 Water-soluble inorganic ions (WSII), consisting of F^- , Cl^- , NO_2^- , NO_3^- , SO_4^{2-} , NH_4^+ , Na^+ , K^+ , Mg^{2+}
65 and Ca^{2+} , are a major component of atmospheric aerosols and can contribute up to 77% of $PM_{2.5}$
66 (particulate matter with aerodynamic diameter $\leq 2.5 \mu m$) mass (Xu et al., 2019a). Secondary inorganic
67 aerosols (SIA) including sulfate, nitrate and ammonium (SNA) often dominate water-soluble ionic
68 species in $PM_{2.5}$, and were reported to account for more than 90% of WSII in Sichuan, China (Tian
69 et al., 2017). In Beijing, the average SNA concentrations can range from $4.2 \pm 2.9 \mu g/m^3$ in non-haze
70 days to $85.9 \pm 22.4 \mu g/m^3$ in heavily polluted days, and contribute 15%-49% of $PM_{2.5}$ (Li et al., 2016).
71 SNA can greatly influence air pollution, visibility, aerosol acidity and hygroscopicity, which are
72 driving factors affecting aerosol-phase pH and chemistry and the uptake of gaseous species by
73 particles (Shon et al., 2012; Xue et al., 2011; Zhang et al., 2019). Hence, the study of WSII is of great
74 interest due to their adverse impacts.

75

76 WSII in aerosols were reported to be analyzed by multiple techniques such as Cl^- by
77 spectrophotometry, and Ca^{2+} and Mg^{2+} by flame atomic absorption in the early 1980s (Harrison and
78 Pio, 1983). However, previous methods were time-consuming as WSII were analyzed by different
79 techniques separately. Ion chromatography (IC), which was first introduced in 1975 (Buchberger,
80 2001), was applied in many studies for routine measurement of atmospheric WSII due to its fast,
81 accurate and sensitive determination in a single run (Heckenberg and Haddad, 1984; Baltensperger
82 and Hertz, 1985). IC can be coupled with diverse detection techniques for ion analysis, such as
83 suppressed conductivity, UV-VIS absorbance, amperometry, potentiometry, mass spectrometry, etc.
84 (Buchberger, 2001). It has been used in various atmospheric studies for many years and is still widely
85 applied at present, such as in the investigation of WSII in size-segregated aerosols (Li et al., 2013;
86 Zhao et al., 2011; Đorđević et al., 2012), fine aerosols (Fan et al., 2017; He et al., 2017; Liu et al.,

87 2017a) and coarse aerosols (Li et al., 2014; Guo et al., 2011; Mkoma et al., 2009). IC can also be used
88 for the determination of both water soluble organic and inorganic ions (Yu et al., 2004; Karthikeyan
89 and Balasubramanian, 2006).

90 Aerosol ion concentrations can also be measured by online methods such as the Aerosol Chemical
91 Speciation Monitor (ACSM) or Aerosol Mass Spectrometer (AMS) (Ng et al., 2011; Sun et al., 2012).
92 During the recent Atmospheric Pollution and Human Health in a Chinese Megacity (APHH-China)
93 campaigns (Shi et al., 2019), we observed important discrepancies between offline aerosol IC
94 observations from different labs and between online AMS and offline IC methods. This prompted us
95 to carry out this intercomparison exercise.

96 The IC method had been validated by a common reference standard - NIST SRM 1648 (urban
97 particulate matter) and the results for Na, K, S and NH_4^+ were compared with those from other
98 suitable alternative analytical techniques such as AAS, UV-VIS and PIXE in previous studies
99 (Karthikeyan and Balasubramanian, 2006). However, to the best of our knowledge, no investigation
100 has been conducted to compare the results of different laboratories (labs) for such an important and
101 widely used simple technique.

102 The aim of this work is to 1) examine the consistency of ion concentrations measured by various labs
103 and by ACSM, 2) explore the impact of the inter-lab variability in ion concentration measurements
104 on aerosol acidity estimates, and 3) provide recommendations for improving future WSII analysis by
105 IC.

106

107 **2. EXPERIMENTAL**

108 **2.1 Participating Laboratories**

109 Ten laboratories from China, United Kingdom and Serbia were invited to take part in the inter-
110 laboratory comparison of atmospheric inorganic ions, which are listed as follows: University of
111 Birmingham; University of York; University of Belgrade; Zhejiang University; Nankai University;

112 Ocean University of China; Beijing Normal University; Chongqing Institute of Green and Intelligent
113 Technology, Chinese Academy of Sciences; Institute of Chemistry, Chinese Academy of Sciences;
114 Institute of Atmospheric Physics, Chinese Academy of Sciences. The participating laboratories were
115 randomly coded from Lab-1 to Lab-10 and not related to the above order.

116

117 **2.2 Sample and Data Collection**

118 Eight daily PM_{2.5} samples were collected on quartz filters (total area: 406.5cm²) from 16th-23rd
119 January 2019 by a high-volume air sampler (1.13 m³ min⁻¹; Tisch Environmental Inc., USA) at an
120 urban site, located at the Institute of Atmospheric Physics (IAP) of the Chinese Academy of Sciences
121 in Beijing, China. The sampling site (116.39E, 39.98N) is located between the North Third Ring Road
122 and North Fourth Ring Road, and approximately 200 m from the G6 Highway. It is 8 m above the
123 ground and surrounded by high-density roads and buildings; detailed information regarding the
124 sampling site can be found elsewhere (Shi et al., 2019). Apart from the aerosol samples, 5 field blank
125 filters were also collected in the same manner with the pump off. All ion concentrations in this study
126 were corrected by the values obtained from field blanks. Hourly PM_{2.5} mass concentrations were
127 obtained from a nearby Olympic Park station, the China National Environmental Monitoring Network
128 (CNEM) website. Shi et al. (2019) showed that the PM_{2.5} data at this station are close to those
129 observed at IAP during the APHH-China campaigns. The close observed PM_{2.5} concentrations at
130 different air quality stations in Beijing provide further reassurance of the representability of the
131 observed concentration at Olympic Park. The original hourly data was averaged to 24 h for better
132 comparison.

133

134 An Aerodyne Time-of-Flight Aerosol Chemical Speciation Monitor (ToF-ACSM) with a PM_{2.5}
135 aerodynamic lens was also deployed on the same roof of the building at IAP for real-time
136 measurements of non-refractory (NR) chemical species (Organics, Cl⁻, NO₃⁻, SO₄²⁻ and NH₄⁺) in

137 PM_{2.5} (NR-PM_{2.5}) with 2 min time resolution (Sun et al., 2020). Another ToF-ACSM was also used
138 to measure the PM_{2.5}-associated non-refractory chemical species at the Beijing University of
139 Chemical Technology (BUCT), which is located at the west third-Ring Road of Beijing and
140 approximately 10 km away from the sampling location of IAP. The collection efficiencies (CE)
141 applied for the ACSM at IAP and BUCT were different. For IAP, a capture vaporizer was used, and
142 the CE was assumed to be close to 1 (Sun et al., 2020). For BUCT, a standard vaporizer was applied
143 with a composition- and acidity-dependent CE calculated according to Middlebrook et al. (2012).
144 Details regarding quality control of the ACSM at IAP and BUCT can be found elsewhere (Sun et al.,
145 2020; Liu et al., 2020). The concentrations of non-refractory species were calculated from mass
146 spectra using a fragmentation table (Allan et al., 2004). The ToF-ACSM data were then averaged to
147 24h for a comparison with those from filter analysis in our study. Note that the ToF-ACSM data at
148 IAP on 19th and 20th and data at BUCT on 17th and 18th are excluded from the comparison due to the
149 maintenance of the instrument. An ammonia analyzer (DLT - 100, Los Gatos Research LGR, USA)
150 which applies a unique laser absorption technology called off-axis integrated cavity output
151 spectroscopy was used for the ambient NH₃ measurements. It has a precision of 0.2 ppb and the
152 original data with 5 min intervals were averaged to 24 h for the calculation of aerosol pH. More
153 information on NH₃ measurement can be found elsewhere (Ge et al., 2019).

154

155 **2.3 Sample Analysis**

156 Filter cuts of 5cm² and 6cm² from the same set of samples were used for extraction in 10 labs. Filters
157 were extracted ultrasonically for 30 minutes with 10 ml ultrapure water in all laboratories and then
158 filtered before IC analysis. The instrument details are given in Table 1 and the extraction details
159 including purity of ultrapure water, model/power of ultrasonicator, type of syringe filter and vials that
160 used for analysis are provided in Table S1. In total, 9 ionic species were reported: F⁻, Cl⁻, SO₄²⁻, NO₃⁻,
161 Na⁺, NH₄⁺, K⁺, Mg²⁺ and Ca²⁺. Other ions including Br⁻, NO₂⁻, PO₄³⁻ and Li⁺ were not included due

162 to their relatively low concentrations in aerosol samples. The calibration detail and QA/QC
 163 procedures are provided in Table S2.

164

165 Certified reference materials (CRM) were also determined for quality control. CRM for cations
 166 (CRM-C, Multi Cation Standard 1 for IC, Sigma-Aldrich) contains 200mg/L Na⁺, 200mg/L K⁺,
 167 50mg/L Li⁺, 200mg/L Mg²⁺, 1000mg/L Ca²⁺ and 400mg/L NH₄⁺. CRM for anion (CRM-A, Multi
 168 Anion Standard 1 for IC, Sigma-Aldrich) contains 3mg/L F⁻, 10mg/L Cl⁻, 20mg/L Br⁻, 20mg/L NO₃⁻,
 169 20mg/L SO₄²⁻ and 30mg/L PO₄³⁻. CRM-C and CRM-A were diluted 180 and 6 times, respectively.
 170 20mL of the diluted CRM solutions were marked as unknown solutions and sent along with the
 171 aerosol samples to each lab for analysis. All CRM solutions were measured by each lab as unknown
 172 samples. All filters and solutions were kept frozen during transportation to prevent any loss due to
 173 volatilization.

174 **Table 1.** Summary of instrument and method details in 10 laboratories.

Lab No.	Instrument model (Ion Chromatograph)		Columns & suppressor		Eluent	
	Anions	Cations	Anions	Cations	Anions	Cations
1	Dionex AQUNION-1100	Dionex AQUNION-1100	IonPac™ AS11-HC separation column; IonPac™ AG11-HC guard column; suppressor ASRS 300	IonPac™ CS12A separation column; IonPac™ CG12A guard column; suppressor CSRS 300;	30 mM KOH; 1.0 ml/min.	20 mM methansulfonic acid; 1.0 ml/min.
2	Dionex ICS-1100	Dionex ICS-1100	IonPac™ AS11-HC separation column; IonPac™ AG11-HC guard column; suppressor ASRS 500	IonPac™ CS12A separation column; IonPac™ CG12A guard column; suppressor CSRS 500	KOH with gradient variation from 0 to 30 mM; 0.38 ml/min.	15 mM methansulfonic acid; 0.25 ml/min
3	Dionex ICS-600	Dionex ICS-600	IonPac™ AS11-HC separation column; IonPac™ AG11-HC guard column; suppressor ASRS 300	IonPac™ CS12A separation column; IonPac™ CG12A guard column; suppressor CSRS 300	20 mM KOH; 1.0 ml/min.	20 mM methansulfonic acid; 1.0 ml/min
4	Dionex 600	Dionex ICS 2100	IonPac™ AS11 separation column; IonPac™ AG11 guard column; suppressor ASRS 300	IonPac™ CS12A separation column; IonPac™ CG12A guard column; suppressor CSRS 300	30 mM KOH; 1.0 ml/min	20 mM methansulfonic acid; 1.0 ml/min
5	Ion Chromatograph (ECO)	Ion Chromatograph (ECO)	Metrosep A5-150 separation column; Metrosep A SUPP 4/5 Guard/4.0 guard column; suppressor MSM	Metrosep C4-150 separation column	3.2 mM Na ₂ CO ₃ -1.0mM NaHCO ₃ ; 0.7 ml/min	1.7 mM nitric acid - 0.7mM dipicolinic acid; 0.9 ml/min
6	Metrohm (940 Professional IC Vario)	Metrohm (940 Professional IC Vario)	Metrohm A SUPP 5-250 separation column; Metrohm A SUPP 10-250 guard column; suppressor MSM-A Rotor	METROSEP C6-150 separation column; Metrohm C4 guard column	3.2 mM Na ₂ CO ₃ -1.0mM NaHCO ₃ ; 0.7 ml/min	1.7 mM nitric acid - 1.7mM dipicolinic acid; 0.9 ml/min

7	Dionex ICS600	Dionex ICS600	IonPac™ AS11-HC separation column; IonPac™ AG11-HC guard column; suppressor ASRS	IonPac™ CS12A separation column; IonPac™ CG12A guard column; suppressor CSRS	30 mM KOH; 1 ml/min	20 mM methansulfonic acid; 1.0 ml/min
8	Dionex ICS-900	Dionex ICS-900	IonPac™ AS14 separation column; IonPac™ AG14 guard column; suppressor Dionex CCRS 500	IonPac™ CS12A separation column; IonPac™ CG12A guard column; suppressor Dionex CCRS 500	3.5 mM Na ₂ CO ₃ -1.0mM NaHCO ₃ ; 1.2 ml/min	20 mM methansulfonic acid; 1.0 ml/min
9	Dionex ICS-1100	Dionex ICS-1100	IonPac™ RFICTM AS14A separation column; IonPac™ RFICTM AG14A Guard column	IonPac™ RFICTM CS12A separation column; IonPac™ RFICTM CG12A Guard column	8.0 mM Na ₂ CO ₃ -1.0mM NaHCO ₃ ; 1.0 ml/min	20 mM methansulfonic acid; 1.0 ml/min
10	Dionex ICS-2100	Dionex INTEGRION HPIC	IonPac™ AS15 separation column; IonPac™ AG15 guard column; suppressor ADRS 600	IonPac™ CS12A separation column; IonPac™ CG12A guard column; suppressor CERS 500;	38mM KOH; 0.3 ml/min.	20 mM methansulfonic acid; 1.0 ml/min.

176 2.4 Coefficient of Divergence Analysis

177 In order to investigate the differences of ionic concentrations measured by different labs, the
178 Pearson's correlation coefficient (R) and the coefficient of divergence (COD) were applied.
179 COD is a parameter to evaluate the degree of uniformity or divergence of two datasets. COD
180 and R were computed for Lab_j/Lab-Median pairs, of which Lab_j indicates the results of each
181 lab and Lab-Median represents the median values of 10 labs. Median values are chosen here to
182 better represent the theoretical true concentrations of the ions, as there are some outliers in
183 some labs, and the averages may be less representative. The results of COD and R were also
184 computed for Lab_j/Lab-Mean, Lab_j/Lab-Upper and Lab_j/Lab-Lower pairs (Supplemental
185 Information Fig. S1-S3), where Lab-Mean, Lab-Upper and Lab-Lower represent the mean
186 value, upper values (84% percentile) and lower values (16% percentile) of ion concentrations
187 measured by 10 labs. COD of ionic concentrations of two datasets is determined as follows:

$$188 \text{COD}_{jk} = \sqrt{\frac{1}{P} \sum_{i=1}^P \left(\frac{X_{ij} - X_{ik}}{X_{ij} + X_{ik}} \right)^2} \quad (1)$$

189 where j represents the ion concentrations measured by an individual lab-j, k stands for the
190 median ion concentrations of 10 labs, P is the number of samples. X_{ij} and X_{ik} represent the
191 concentration of ion i measured by lab-j and the median concentration of ion i measured by 10
192 labs, respectively. COD value equal to 0 implies no difference between two datasets, while a
193 COD of 1 means absolute heterogeneity and maximum difference between two datasets (Liu
194 et al., 2017c). A COD value of 0.2 is applied as an indicator for similarity and variability
195 (Krudysz et al., 2008). A higher COD (>0.2) implies variability between two datasets, while
196 lower COD (<0.2) indicates similarity between them. Overall, lower COD (<0.2) and higher R
197 (>0.8) of the lab suggest the similar variation pattern and similar ion concentrations of this lab
198 with the median values of 10 labs.

199

200 2.5 ISORROPIA-II

201 ISORROPIA-II is a thermodynamic equilibrium model for predicting the composition and
202 physical state of atmospheric inorganic aerosols (available at <http://isorrophia.eas.gatech.edu>)
203 (Fountoukis and Nenes, 2007). It was applied in this study to calculate the aerosol water content
204 (AWC) and pH. Aerosol pH in this study (pH_i) was defined as the molality-based hydrogen ion
205 activity on a logarithmic scale, calculated applying the following equation (Jia et al., 2018;
206 Song et al., 2019):

$$207 \text{pH}_i = -\log_{10} \left(a_{\text{H}^+_{(\text{aq})}} \right) = -\log_{10} \left(m_{\text{H}^+_{(\text{aq})}} \gamma_{\text{H}^+_{(\text{aq})}} / m^\ominus \right) \quad (2)$$

208 where $a_{\text{H}^+_{(\text{aq})}}$ represents hydrogen ion activity in aqueous solution, $\text{H}^+_{(\text{aq})} \cdot m_{\text{H}^+_{(\text{aq})}}$ and $\gamma_{\text{H}^+_{(\text{aq})}}$
209 represent the molality and the molality-based activity coefficient of $\text{H}^+_{(\text{aq})}$, respectively. m^\ominus is
210 the standard molality (1 mol kg^{-1}). Model inputs include aerosol-phase Cl^- , SO_4^{2-} , NO_3^- , Na^+ ,
211 NH_4^+ , K^+ , Mg^{2+} , Ca^{2+} and gas-phase NH_3 concentrations, along with daily averaged
212 temperature and relative humidity (Table S3). In this study, the model was run only in forward
213 mode (with gas + aerosol inputs) in the thermodynamically metastable phase state,
214 assuming salts do not precipitate under supersaturated conditions. More information regarding
215 applications of ISORROPIA-II can be found in other studies (Guo et al., 2016; Weber et al.,
216 2016; Song et al., 2018).

217

218 3. RESULTS AND DISCUSSION

219 3.1 Quality Assurance and Quality Control (QA & QC)

220 3.1.1 Certified reference materials (CRM) – detection accuracy and repeatability

221 Certified reference materials for both cations and anions were investigated for quality control.
222 CRM-C and CRM-A were analyzed three consecutive times in each lab. The detection

223 accuracy (DA) of each ion was determined as the ratio of measured concentration divided by
 224 its certified concentration in percentage. The results of DA of all ions are listed in Table 2.

225 **Table 2.** Detection accuracy (%) of water-soluble inorganic ions in certified reference materials
 226 measured by 10 laboratories.

Lab NO.	F ⁻	Cl ⁻	SO ₄ ²⁻	NO ₃ ⁻	Na ⁺	NH ₄ ⁺	K ⁺	Mg ²⁺	Ca ²⁺
1	111.8 ± 0.2	107.6 ± 0.1	108.5 ± 2.4	110 ± 0.5	98.2 ± 0.0	108.7 ± 0.3	99.4 ± 0.2	95.6 ± 0.3	99.6 ± 0.6
2	89.1 ± 0.4	95.1 ± 0.2	94.0 ± 1.0	94.5 ± 0.5	102.2 ± 1.0	135.0 ± 6.0	94.9 ± 4.6	95.9 ± 0.2	92.8 ± 0.5
3	101 ± 1.4	95.9 ± 0.3	132.4 ± 31.4	97.1 ± 1.0	91.4 ± 0.1	93.5 ± 0.2	92.4 ± 0.2	105.5 ± 0.3	98.7 ± 0.4
4	94.1 ± 4.0	90.4 ± 0.2	91.9 ± 1.2	91.7 ± 1.4	93.3 ± 1.7	112.2 ± 0.6	92.0 ± 2.8	98.9 ± 2.0	100.4 ± 1.1
5	94.0 ± 3.1	99.0 ± 0.0	92.4 ± 0.9	97.7 ± 0.0	85.9 ± 3.2	89.3 ± 0.5	92.1 ± 4.9	96.1 ± 0.6	101.7 ± 3.0
6	93.3 ± 0.3	110.8 ± 0.5	89.2 ± 0.1	91.4 ± 0.2	98.2 ± 1.1	88.4 ± 1.1	92.2 ± 4.9	102.0 ± 2.1	102.6 ± 1.2
7	89.4 ± 2.7	114.5 ± 21.3	100.8 ± 0.0	105.2 ± 0.2	97.0 ± 1.3	107.5 ± 0.8	72.1 ± 0.8	93.5 ± 0.4	91.9 ± 1.1
8	92.0 ± 0.0	96.6 ± 0.7	97.4 ± 1.1	96.2 ± 1.2	97.3 ± 0.0	93.8 ± 0.3	97.3 ± 0.9	94.0 ± 2.1	89.3 ± 0.6
9	102.6 ± 1.5	105.9 ± 1.0	101.9 ± 4.5	99.1 ± 3.5	101.2 ± 0.1	110.6 ± 0.2	103.0 ± 0.0	99.7 ± 0.2	102.2 ± 0.3
10	103.4 ± 1.6	103.5 ± 0.7	99.0 ± 9.3	114.2 ± 2.5	95.3 ± 4.1	91.0 ± 4.1	91.5 ± 4.7	94.8 ± 3.8	96.3 ± 2.1

227

228 As reported in Table 2, most ions were observed with DA in the range 90% - 110% among 10
 229 laboratories. However, SO₄²⁻ in Lab-3 and NH₄⁺ in Lab-2 were overestimated, the DA of which
 230 were 132.4%±31.4% and 135.0%±6.0%, respectively. The standard deviation of SO₄²⁻
 231 measured by Lab-3 was the largest (31.4%), followed by Cl⁻ measured by Lab-7 (21.3%),
 232 which indicated their poor repeatability. Even though NH₄⁺ in Lab-2 was observed with high
 233 value of DA, its deviation of three repeats was relatively small, which may be attributable to
 234 the evaporation of ammonium in calibration standards in Lab-2; hence, the level it represented
 235 was higher than its real concentration. K⁺ in Lab-7 was underestimated, and was observed with
 236 a DA of only 72.1%±0.8%. This may be due to contamination in the water blanks or the IC
 237 system, as the average concentration of K⁺ in 3 water blanks of Lab-7 was 8.0 ng/L, much
 238 higher than the median value of 10 labs (3.4 ng/L).

239

240 3.1.2 Detection limits

241 The detection limits (DLs) in this study were calculated as:

242 $DL = 3 \times SD_i$ (3)

243 where SD_i is the standard deviation of the blank filters. The mean concentrations of the ions in
 244 blanks and DLs (3SD) of all ions are provided in Table 3.

245 **Table 3.** Mean filter blank concentrations and detection limits (3SD) (ng/m³) of ions measured by 10
 246 laboratories.

Lab	F ⁻		Cl ⁻		SO ₄ ²⁻		NO ₃ ⁻		Na ⁺		NH ₄ ⁺		K ⁺		Mg ²⁺		Ca ²⁺	
	mean	3SD	mean	3SD	mean	3SD	mean	3SD	mean	3SD	mean	3SD	mean	3SD	mean	3SD	mean	3SD
1	2.3	4.0	33.2	31.5	74.2	12.7	64.2	7.1	78.3	31.3	37.2	16.6	7.9	19.6	3.4	3.9	50.0	18.2
2	0.2	0.4	10.9	11.3	15.6	2.5	35.3	14.7	11.5	8.0	20.8	5.0	3.4	1.2	3.2	6.8	38.1	54.6
3	2.8	2.0	6.3	2.7	8.7	11.7	15.3	10.5	0.5	3.4	9.6	3.9	0.0	0.0	0.0	0.0	6.8	18.8
4	59.6	195.2	103.6	229.3	85.3	25.9	50.3	159.6	22.8	29.4	59.6	123.2	19.1	26.5	10.1	1.9	376.4	90.4
5	4.2	2.7	50.9	98.6	33.4	40.8	25.7	116.5	51.6	57.7	46.3	54.7	22.6	9.4	45.4	9.4	268.2	49.8
6	n.a.	n.a.	251.6	7.4	55.1	53.6	24.5	0.0	56.6	35.9	35.0	46.1	n.a.	n.a.	n.a.	n.a.	n.a.	n.a.
7	2.1	3.9	11.4	11.8	37.9	32.7	14.5	40.3	6.1	0.0	5.8	0.0	4.9	12.4	1.4	4.5	7.6	17.3
8	n.a.	n.a.	29.0	32.8	17.4	26.1	n.a.	n.a.	8.7	22.6	n.a.	n.a.	n.a.	n.a.	n.a.	n.a.	20.3	27.1
9	n.a.	n.a.	n.a.	n.a.	34.8	32.8	39.5	22.7	47.4	12.1	21.2	8.3	10.1	5.4	1.6	0.2	7.1	32.4
10	29.4	1.3	19.5	21.1	59.4	21.3	78.8	102.2	24.6	53.3	33.5	34.2	31.3	82.1	4.3	0.0	10.2	14.6

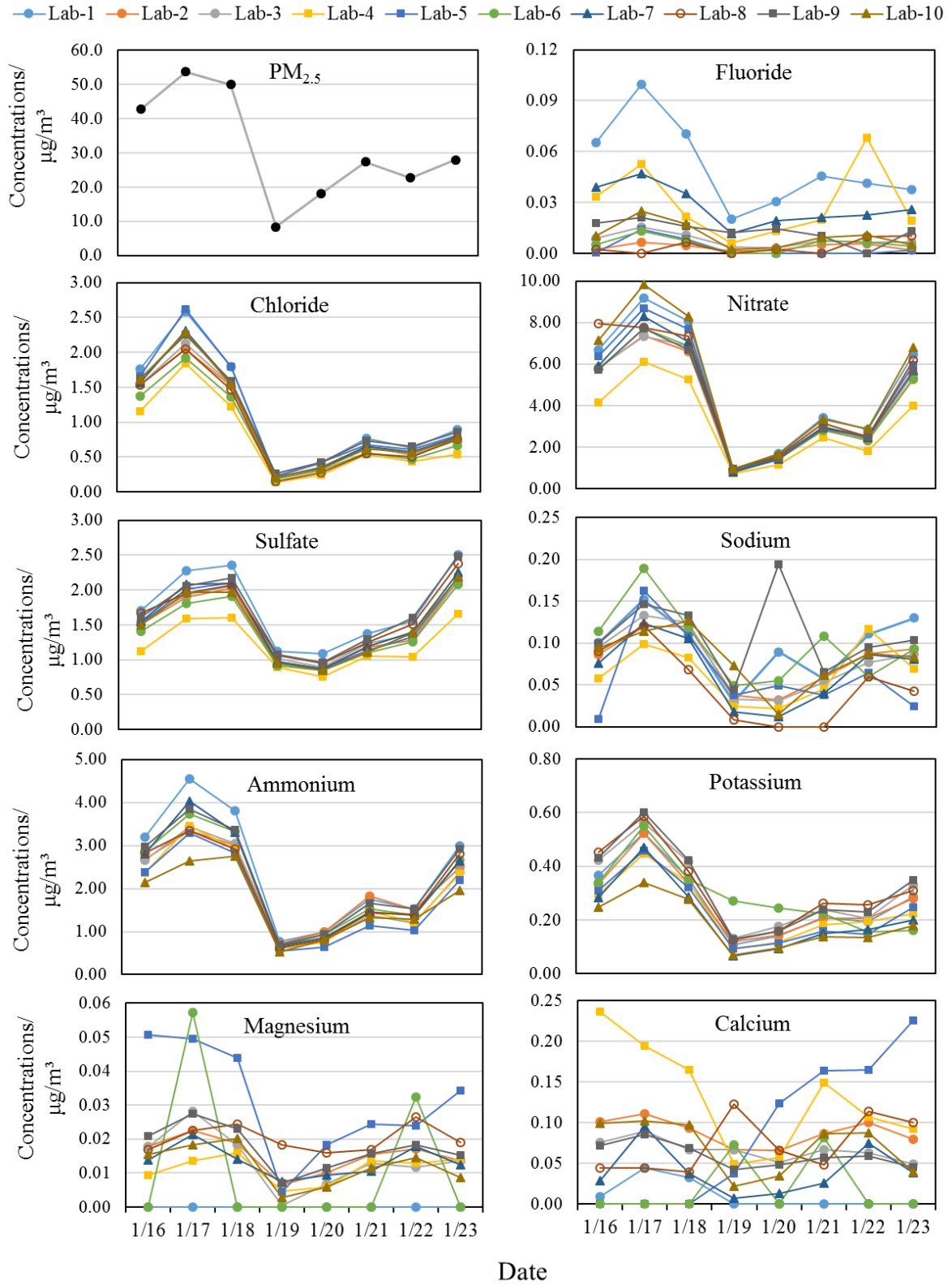
247 *Note: The detection limits were calculated based on large-volume sampling (total filter size: 406.5 cm²; total*
 248 *sampling volume: 1560 m³); n.a.: not available due to no relevant peaks being identified in the chromatography.*

249 **3.2 Mass Concentrations of PM_{2.5} and Inorganic Ions**

250 **3.2.1 PM_{2.5} and ion concentrations**

251 The results for PM_{2.5} and all inorganic ion concentrations measured by 10 labs are presented in
252 Fig. 1. During January 16th – 23rd 2019, the daily mean PM_{2.5} ranged from 8.4 to 53.8 µg/m³,
253 with an average of 31.4 µg/m³. Among them, January 16th, 17th and 18th were deemed
254 moderately polluted days with PM_{2.5} concentration > 35 µg/m³, while the rest were non-haze
255 days with PM_{2.5} concentrations falling in the range of 8.4-27.9 µg/m³.

256



257

258

Fig. 1 The time series of mass concentrations of PM_{2.5} and ions

259

260 The time series of all inorganic ions are also shown in Fig. 1 to demonstrate the consistency
261 among different laboratories. In Fig. 1, Cl^- , NO_3^- , SO_4^{2-} and NH_4^+ showed a similar trend to
262 $\text{PM}_{2.5}$ and good correlations among the 10 labs, suggesting the consistency and reliability of
263 using Ion Chromatography for analysing these ions, despite various instruments and analysing
264 methods. Larger variations of Cl^- , NO_3^- , SO_4^{2-} and NH_4^+ concentrations between different
265 laboratories were observed in moderately polluted days, whereas results for the non-haze days,
266 especially for 19th and 20th, were observed with good agreement in 10 labs. Good agreement
267 was also observed for the mass ratios of $\text{NO}_3^-/\text{SO}_4^{2-}$ in most of the labs during the study period
268 (Fig. S4), which basically followed a similar trend as $\text{PM}_{2.5}$. On more polluted days,
269 $\text{NO}_3^-/\text{SO}_4^{2-}$ ratios were obviously higher than less polluted days, suggesting the dominance of
270 mobile source contributions over stationary sources during heavily polluted days.

271

272 The average SNA concentrations of 8 samples varied from 6.3 ± 3.3 (Lab-4) to 9.1 ± 5.0 (Lab-1)
273 $\mu\text{g}/\text{m}^3$ in 10 labs, accounting for 20.6 ± 4.8 % to 29.0 ± 6.7 % of the $\text{PM}_{2.5}$ mass concentrations.
274 However, their contributions to total ions measured by each lab were not significantly different,
275 which ranged between $83.6 \pm 2.7\%$ and $86.3 \pm 2.3\%$. The total ions summed to $24.3 \pm 4.9\%$ (Lab-
276 4) to $33.8 \pm 7.1\%$ (Lab-1) of $\text{PM}_{2.5}$. These results are comparable with those in another study in
277 Beijing which found that SNA accounted for 88% of total ions and 9-70% of $\text{PM}_{2.5}$
278 concentrations (Xu et al., 2019b). As shown in Table 2, the DA of most ions measured by Lab-
279 4 were $< 100\%$, while those of Lab-1 were much higher, especially for major ions ($>100\%$).
280 Corresponding to this, the ion concentrations in Lab-4 were mostly lower than other labs, while
281 those of Lab-1 were mostly higher than other labs. For Lab-6 which was also observed to have
282 lower DA of ions such as SO_4^{2-} (89.2%) and NH_4^+ (88.4%) in 10 labs; its SNA concentrations
283 and total ions accounted for 24.5 ± 5.6 % and $28.7 \pm 6.0\%$ of $\text{PM}_{2.5}$, respectively, the second

284 lowest among all labs. Hence, it is very important to run certified reference materials before
285 any sample analysis to ensure accuracy and good quality of data.

286

287 K^+ concentrations analysed by 10 labs followed a similar trend to $PM_{2.5}$ mass, except the
288 sample measured on a moderately polluted day (19th) by Lab-6, which is 2-3 times higher than
289 that measured by other labs. F^- concentrations varied across 10 labs, but most of them shared
290 a similar trend. Some labs like Lab-8 did not follow the same trend due to reporting
291 undetectable F^- concentrations. The Na^+ concentration on the least polluted day (20th) was
292 abnormally high in Lab-9, while its concentrations measured by other labs were generally low.
293 This could be due to Na^+ contamination during preparation or measurement of this sample, as
294 Na^+ concentrations in the rest of the samples measured by Lab-9 followed a similar trend as
295 that of other labs. The alkaline ions Mg^{2+} and Ca^{2+} are mostly originated from crustal dust and
296 mainly exist in coarse particles (Zou et al., 2018). Their mass concentrations varied
297 considerably due to their relatively low concentrations in aerosol samples and being sometimes
298 below the detection limits in some labs, such as Lab-6. Nevertheless, some labs like Lab-2, 3,
299 and 10 still followed a similar trend.

300

301 **3.2.2 Comparison with ToF-ACSM data**

302 As shown in Fig. 1, Cl^- , NO_3^- , SO_4^{2-} , NH_4^+ generally exhibited similar patterns, but due to
303 some outliers, such as NO_3^- concentration measured by Lab-8 on the 16th, the median values
304 were selected to better represent the general levels and theoretical actual concentrations of ions
305 measured by different labs. The scatter plots of the median mass concentrations of Cl^- , NO_3^- ,
306 SO_4^{2-} and NH_4^+ in 10 labs (IC- Cl^- , NO_3^- , SO_4^{2-} and NH_4^+) *versus* the non-refractory (NR)
307 species measured by the ToF-ACSM (ACSM- Cl^- , NO_3^- , SO_4^{2-} and NH_4^+) are shown in Fig. 2.
308 The time series of IC and ACSM data at IAP and BUCT are plotted in Fig. S5.

309 Chloride is reported to arise mainly from biomass burning and coal combustion in China
310 (Zhang et al., 2016). Its average concentration in 10 labs correlated very well with ACSM-Cl⁻
311 ($R^2=0.82$ for IAP). However, IC-Cl⁻ in IAP is 2-3 times higher than ACSM-Cl⁻; this may be
312 due to the small contribution of Cl⁻ to the overall mass spectrum which made it difficult to
313 quantify by ToF-ACSM (Allan et al., 2004). Additionally, the ACSM is incapable of measuring
314 Cl⁻ in the form of KCl, as the ACSM only measures non-refractory Cl⁻. Poor correlation of
315 chloride ($R^2=0.21$) was also discovered between two collocated ACSMs with a much larger set
316 of data points, while other NR species were observed with strong correlation ($R^2>0.8$) in
317 another study (Budisulistiorini et al., 2014), suggesting the quantification of chloride by ACSM
318 has large uncertainties.

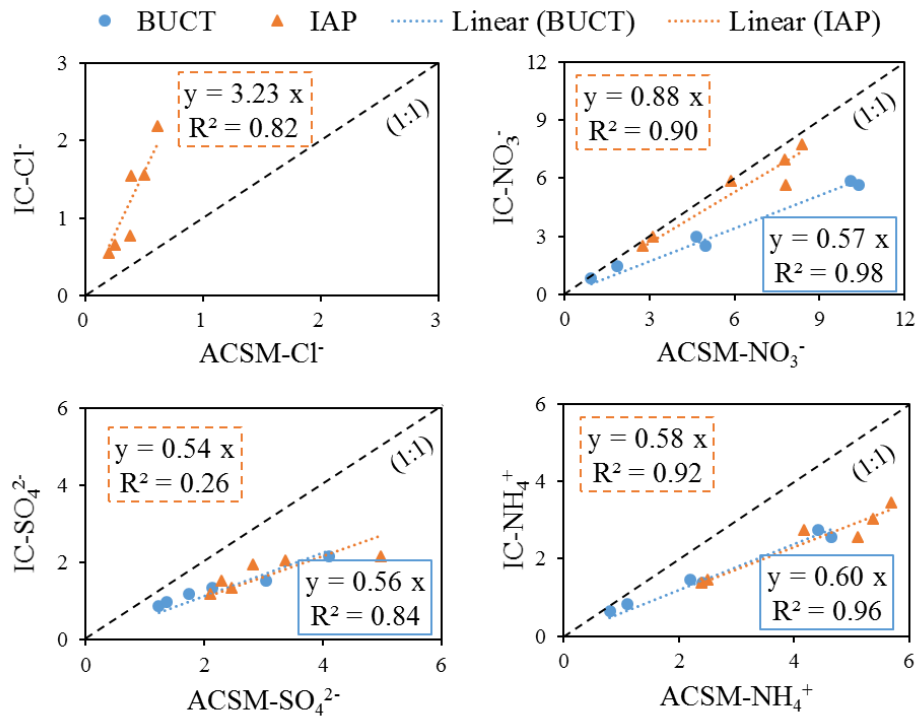
319 Sulfate, as another important component of atmospheric secondary inorganic aerosols, plays
320 an important role in the formation of haze (Wang et al., 2014; Yue et al., 2019). The correlation
321 coefficient (R^2) between the measured IC-SO₄²⁻ and ACSM-SO₄²⁻ was only 0.26 for IAP with
322 a slope of 0.54. The correlation of IC-SO₄²⁻ and ACSM-SO₄²⁻ from BUCT was 0.84 (R^2) with
323 a slope of 0.56. Judging from the slopes, ACSM-SO₄²⁻ and ACSM- NH₄⁺ were similarly higher
324 than the median values of measured SO₄²⁻ and NH₄⁺ concentrations in this study. The NR
325 species followed the same trend as NR-PM_{2.5}, and chemical species measured through filter
326 analysis also shared the same trend as PM_{2.5} measured in our study.

327 Very good correlation between measured IC and ACSM data was found for NO₃⁻ and NH₄⁺
328 with $R^2>0.9$. The lab median value of NO₃⁻ was very close to the ACSM-NO₃⁻ from the same
329 sampling site- IAP, with a slope of 0.88 for IC-NO₃⁻/ ACSM-NO₃⁻, while that of BUCT was
330 only 0.57. The slopes of IC-NH₄⁺/ ACSM-NH₄⁺ were 0.58 and 0.60 for IAP and BUCT,
331 respectively. Comparing IC-NH₄⁺ to ACSM-NH₄⁺, the absolute concentration of IC-NH₄⁺
332 differed the most among all ions (42%), except Cl⁻. Generally, ACSM-NO₃⁻ and ACSM-NH₄⁺
333 were higher than the median values of measured NO₃⁻ and NH₄⁺ concentrations in the 10 labs.

334 Higher concentrations in the online ACSM observations compared to the daily filter sample
335 measurements may be partially due to differences in the performance of the two PM_{2.5} cut-
336 point selectors, which lead to different transmission efficiency of particles. Other reasons could
337 be: 1) the uncertainties in ACSM observations themselves. Crenn et al. (2015) reported the
338 uncertainties of NO₃⁻, SO₄²⁻, and NH₄⁺ in ACSM analysis were 15%, 28%, and 36%,
339 respectively; 2) negative filter artefacts, such as volatilization of semi-volatile ions (Kim et al.,
340 2015), although that the latter would not be expected to affect sulfate. Sun et al. (2020) also
341 compared ACSM and filter based IC results and showed that the concentrations of NO₃⁻, NH₄⁺
342 and SO₄²⁻ in the ACSM measurement were also higher than those of filter-based, although the
343 slopes were smaller than in our study. It is also possible that the representative ions of ACSM-
344 NO₃⁻ and -NH₄⁺ could have significant interferences from other species in the mass spectrum,
345 causing large uncertainties even after correction for those interferences.

346 To summarize, SO₄²⁻, NO₃⁻, NH₄⁺ from lab analysis generally correlated very well with the
347 ACSM data, but the absolute concentrations differ by up to 42%. Cl⁻ from the two methods is
348 correlated but the concentration differ by more than a factor of three. It appears that Cl⁻ is less
349 accurate in online ACSM observations. NO₃⁻ was comparable for the online data and filter-
350 based data, while SO₄²⁻ and NH₄⁺ in online data may be generally overestimated by a similar
351 factor. It should be noted that higher SO₄²⁻ concentrations in online ACSM data could
352 potentially be due to ACSM not being able to separate organosulfate from sulfate. ACSM-NO₃⁻,
353 -SO₄²⁻ and -NH₄⁺ were also reported to be higher (approximately 10-20%) than filter analysis
354 based NO₃⁻, SO₄²⁻ and NH₄⁺ in another study (Sun et al., 2020). Although the comparison
355 between IC and ACSM provided important information about the data from the two methods,
356 we recognize that we only have 8 data points here. Future studies should be carried out and
357 include more data points in order to comprehensively study the relationship between the online

358 ACSM data and filter-based data. We emphasize that it is essential that both ACSM and filter-
 359 based observations are robustly quality controlled before any ACSM and IC intercomparison.
 360



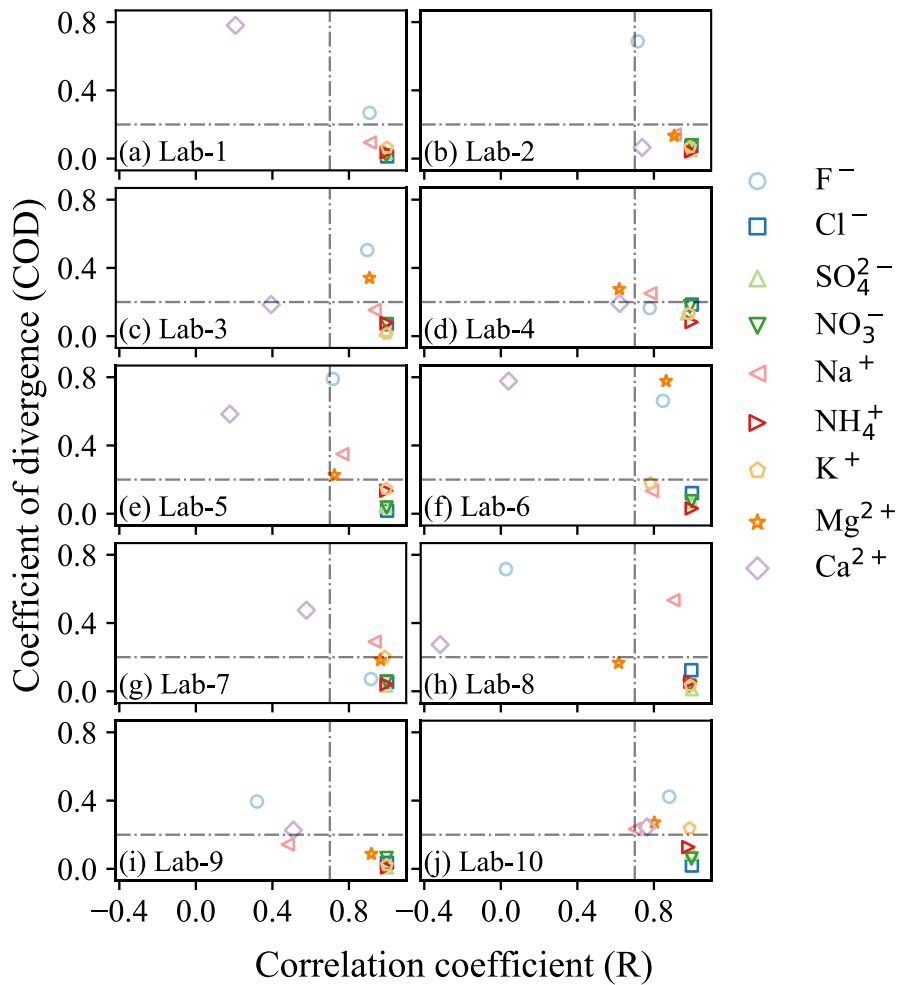
361
 362 **Fig. 2** Scatter plots of the median mass concentrations of Cl^- , NO_3^- , SO_4^{2-} and NH_4^+ measured
 363 by 10 labs (IC- Cl^- , NO_3^- , SO_4^{2-} and NH_4^+) versus the non-refractory (NR) chemical species
 364 from ACSM (ACSM- Cl^- , NO_3^- , SO_4^{2-} and NH_4^+) from BUCT and IAP.

365

366 3.3 Divergence and Correlation Analysis

367 As shown above, some ions like Cl^- , NO_3^- , SO_4^{2-} , NH_4^+ generally exhibited similar patterns,
 368 but some of the ions varied significantly in different laboratories. Therefore, the Pearson's
 369 correlation coefficient (R) and the coefficient of divergence (COD) were both calculated to
 370 identify the uniformity and divergence of ionic concentrations measured by different labs. The
 371 COD and R values of all ions for Lab_j/Lab-Median pairs are presented in Fig. 3. Cl^- , NO_3^- ,
 372 SO_4^{2-} , NH_4^+ and K^+ clearly showed high R values (>0.8) and low COD values (<0.2) in all
 373 labs, suggesting the reliability of the measurement of these ions in different labs. However, F^-
 374 and Ca^{2+} in most labs was observed with higher COD values, and Ca^{2+} was also found with

375 lower R, suggesting heterogeneity of Ca^{2+} detection in different labs, which made this ion less
 376 reliable. Mg^{2+} was observed with good correlation (>0.7) between each lab and the Lab-Median,
 377 but a higher COD was found between Lab-3, 5, 6 with the Lab-Median. Similarly, Na^+ was
 378 also observed with good correlation (>0.7) between each lab and the Lab-Median, except Lab-
 379 9, and a higher COD was found between Lab-5, 8 with the Lab-Median.



380
 381 **Fig. 3** Coefficient of divergence (COD) plotted against correlation coefficient (R) for all ions
 382 in each lab with the median ionic concentrations of 10 labs. (Note: vertical line indicates an R
 383 value of 0.8, and horizontal lines indicate COD values of 0.2).

384
 385 **3.4 Ion Concentrations calculated by Detection Accuracy of CRM**

386 The detection accuracy of the certified reference materials was used to correct the ion
 387 concentrations in this study to show the importance of using CRM for calibration check and

388 quality control. The correction was conducted by dividing the measured ion concentrations by
389 their corresponding DA value. The coefficient of variation (CV) which can indicate the
390 variance of data, was applied here to compare the variation of uncorrected/corrected ion
391 concentrations among 10 labs. It was calculated as the standard deviation of ion concentrations
392 measured by 10 labs divided by the mean and expressed in a percentage. A lower CV value
393 indicates the closeness of data measured by 10 labs and reflects more precise results, while
394 higher CV value reflects the opposite. As F^- , Na^+ , Mg^{2+} and Ca^{2+} were undetectable in some
395 labs, only Cl^- , SO_4^{2-} , NO_3^- , NH_4^+ and K^+ were investigated and the results are shown in Table
396 4.

397

398 In Table 4, Lab-7 was excluded from the calculation of CV of both uncorrected and corrected
399 chloride, due to its poor repeatability. The CV of uncorrected chloride concentration in 8
400 samples varied between 11.7-19.3%, with an average of 14.3%. CV of corrected chloride
401 concentration in 8 samples varied between 10.4-17.0%, with an average of 12.6%. The
402 averaged CV decreased 1.7% for corrected chloride concentration. Small changes of CV were
403 observed during moderately polluted days (16th, 17th, 18th), but more obvious changes occurred
404 during non-haze days.

405

406 The average CV of SO_4^{2-} surprisingly increased from 9.8% for uncorrected to 10.9% for
407 corrected SO_4^{2-} (Supplemental Table S4). However, when excluding Lab-3 from the
408 calculation, the averaged CV of uncorrected sulfate concentration was 10.3% and it
409 significantly decreased to 6.9% once corrected. Therefore, it is strongly recommended that
410 excessive DA (>110%) with large variation should be avoided for the correction of SO_4^{2-}
411 concentrations. Better agreements of NO_3^- and K^+ concentrations among 10 labs were also

412 observed after correction, as indicated by lower CV values for corrected samples. Similar to
 413 other ions, the mean concentration of NH_4^+ of the 10 labs remained almost the same after
 414 correction, but the CV of corrected samples increased from 12.5% to 13.2% after correction
 415 (Table S4). Nevertheless, it decreased 1.2% after correction when excluding Lab-2 (the DA of
 416 NH_4^+ was 135.0 ± 6.0 %) from the calculation. The small change of coefficient of variation here
 417 could be due to the high volatility of ammonia which leads to differing results measured by
 418 different analytical procedures in labs.

419

420 To sum up, certified reference materials should be applied for the quality control. If the values
 421 of DA are highly deviated from 100% (e.g., >110% or <90%) or there is large inter-CRM
 422 variations, then the measurement procedures have to be checked, including repeating the
 423 analysis or re-preparing the calibration standard solutions.

424

425 **Table 4.** Uncorrected and CRM-corrected ion concentrations ($\mu\text{g}/\text{m}^3$) and their corresponding
 426 coefficient of variations (CV/ %).

	Uncorrected Mean (min- max)	CV/%	Corrected Mean (min- max)	CV/%	Uncorrected Mean (min- max)	CV/%	Corrected Mean (min- max)	CV/%
	<u>Chloride</u>				<u>Sulfate</u>			
2019/1/16	1.5 (1.2-1.8)	11.7	1.5 (1.2-1.7)	10.4	1.5 (1.1-1.7)	11.3	1.6 (1.2-1.7)	8.8
2019/1/17	2.2 (1.8-2.6)	12.4	2.2 (1.7-2.6)	11.3	2.0 (1.6-2.3)	9.7	2.0 (1.7-2.2)	6.0
2019/1/18	1.5 (1.2-1.8)	11.9	1.5 (1.2-1.8)	11.2	2.0 (1.6-2.4)	10.2	2.1 (1.7-2.3)	7.3
2019/1/19	0.2 (0.1-0.3)	19.3	0.2 (0.2-0.2)	16.8	1.0 (0.9-1.1)	7.9	1.0 (1.0-1.1)	4.5
2019/1/20	0.3 (0.2-0.4)	19.0	0.3 (0.3-0.4)	17.0	0.9 (0.8-1.1)	10.7	0.9 (0.8-1.0)	6.7
2019/1/21	0.6 (0.5-0.8)	12.6	0.6 (0.5-0.7)	11.0	1.2 (1.1-1.4)	8.7	1.2 (1.1-1.3)	4.7
2019/1/22	0.5 (0.4-0.7)	13.4	0.5 (0.4-0.6)	11.3	1.4 (1.0-1.6)	12.5	1.4 (1.1-1.6)	8.8
2019/1/23	0.8 (0.5-0.9)	13.9	0.8 (0.6-0.8)	12.0	2.2 (1.7-2.5)	11.6	2.3 (1.8-2.4)	8.5
Average		14.3		12.6		10.3		6.9
	<u>Nitrate</u>				<u>Ammonium</u>			
2019/1/16	6.1 (4.1-8.0)	16.5	6.1 (4.5-8.3)	15.2	2.7 (2.1-3.2)	12.7	2.7 (2.1-3.2)	12.8
2019/1/17	8.0 (6.1-9.8)	13.1	8.0 (6.7-8.9)	7.8	3.6 (2.6-4.5)	14.9	3.6 (2.9-4.2)	12.1
2019/1/18	7.1 (5.3-8.3)	12.1	7.1 (5.7-7.9)	8.4	3.1 (2.7-3.8)	10.8	3.2 (2.6-3.8)	10.2
2019/1/19	0.9 (0.7-0.9)	8.9	0.9 (0.8-1.0)	7.3	0.6 (0.5-0.8)	11.7	0.6 (0.6-0.7)	9.4
2019/1/20	1.5 (1.2-1.7)	9.8	1.5 (1.3-1.6)	7.0	0.8 (0.6-1.0)	13.1	0.8 (0.7-1.1)	13.3
2019/1/21	3.0 (2.4-3.4)	9.4	3.0 (2.7-3.3)	5.9	1.5 (1.1-1.7)	12.1	1.5 (1.3-1.7)	9.7

2019/1/22	2.4 (1.8-2.9)	12.3	2.5 (2.0-2.6)	7.9	1.3 (1.0-1.5)	12.3	1.3 (1.1-1.6)	11.8
2019/1/23	5.7 (4.0-6.8)	13.6	5.7 (4.4-6.4)	9.6	2.5 (2.0-3.0)	13.7	2.6 (2.1-3.0)	12.6
Average		12.0		8.6		12.7		11.5
	Potassium							
2019/1/16	0.3 (0.2-0.5)	19.8	0.4 (0.3-0.5)	16.2				
2019/1/17	0.5 (0.3-0.6)	15.6	0.5 (0.4-0.7)	14.9				
2019/1/18	0.3 (0.3-0.4)	14.1	0.4 (0.3-0.5)	10.8				
2019/1/19	0.1 (0.1-0.3)	48.5	0.1 (0.1-0.3)	47.7				
2019/1/20	0.1 (0.1-0.2)	31.4	0.2 (0.1-0.3)	29.7				
2019/1/21	0.2 (0.1-0.3)	20.9	0.2 (0.2-0.3)	17.0				
2019/1/22	0.2 (0.1-0.3)	20.6	0.2 (0.1-0.3)	17.8				
2019/1/23	0.3 (0.2-0.3)	25.3	0.3 (0.2-0.4)	21.3				
Average		24.5		21.9				

427 *Lab-2, 3 and 7 were excluded for calculating CV% of ammonium, sulfate and chloride, respectively.*

428

429 **3.5 Aerosol Acidity**

430 In this study, aerosol acidity was evaluated applying three different parameters: Anion and
431 Cation Equivalence Ratio, ion-balance and in situ acidity. Ion-balance was calculated by
432 subtracting equivalent cations from anions (Zhang et al., 2007), while in-situ aerosol acidity
433 was represented by pH or the concentration of free H⁺ in the deliquesced particles under
434 ambient conditions. In situ aerosol pH can be estimated from various thermodynamic models,
435 for example, SCAPE, GFEMN, E-AIM and ISORROPIA (He et al., 2012; Pathak et al., 2009;
436 Yao et al., 2006). In situ aerosol acidity is most likely to influence the chemical behavior of
437 aerosols (He et al., 2012). Ion-balance is widely used to indicate the neutralization status of
438 aerosols with the equivalent ratios of anions/cations in a relative way (Sun et al., 2010; Takami
439 et al., 2007; Chou et al., 2008). It is noteworthy that ion-balance and in-situ aerosol acidity
440 estimations are empirical approaches which are strongly dependent on the selection of ion
441 species.

442

443 **3.5.1 Anion and Cation Equivalence Ratio**

444 The ratio of the anion molar equivalent concentrations to the cation molar equivalent
 445 concentrations (AE/CE) can be applied to reflect the potential aerosol acidity (Meng et al.,
 446 2016; Zou et al., 2018). In this study, AE and CE were calculated as:

447
$$AE = [SO_4^{2-}/96] \times 2 + [NO_3^-/62] + [Cl^-/35.5] + [F^-/19] \quad (4)$$

448
$$CE = [NH_4^+/18] + [Na^+/23] + [K^+/39] + [Mg^{2+}/24] \times 2 + [Ca^{2+}/40] \times 2 \quad (5)$$

449

450 AE represents the equivalent concentrations of all anions; and CE denotes all cations equivalent
 451 concentrations.

452 **Table 5.** Anion and cation equivalent ratios (AE/CE) among 10 laboratories.

453

	Lab-1	Lab-2	Lab-3	Lab-4	Lab-5	Lab-6	Lab-7	Lab-8	Lab-9	Lab-10
2019/1/16	1.02	1.01	1.02	0.81	1.26	0.93	1.03	1.18	0.93	1.43
2019/1/17	1.00	1.02	1.01	0.85	1.25	0.93	0.87	1.07	0.96	1.59
2019/1/18	1.03	1.03	1.04	0.84	1.26	0.96	1.03	1.14	0.95	1.28
2019/1/19	0.99	0.79	0.97	0.85	1.11	0.65	0.99	0.90	0.98	1.15
2019/1/20	1.00	0.80	0.96	0.85	1.14	0.82	1.00	0.98	0.83	1.08
2019/1/21	1.03	0.78	1.03	0.80	1.14	0.85	1.04	1.02	0.90	1.12
2019/1/22	1.04	0.79	1.04	0.80	1.16	0.90	0.97	0.91	0.93	1.09
2019/1/23	1.02	0.98	1.05	0.80	1.15	0.95	0.84	1.00	0.94	1.48

454

455 As presented in Table 5, the AE/CE ratio of all samples were compared among 10 labs. The
 456 ratios in Lab-1 and Lab-3 were close to unity. The ratios in Lab-5 and Lab-10 were above 1,
 457 indicating the deficiency of cations to neutralize all anions, while that was the contrary of Lab-
 458 4, 6 and 9. In Table 2, the detection accuracies of major cations (Na⁺, NH₄⁺, K⁺) were <100%
 459 and much lower than those of the major anions (Cl⁻, NO₃⁻, SO₄²⁻) in Lab-5 and 10, which may
 460 have caused lower cation concentrations than their real concentrations and a constant higher
 461 ratio of AE/CE. For Lab-9, the detection accuracies of all ions were very close to 100%, except

462 NH_4^+ which was found with a detection accuracy of >110%. Therefore, $\text{AE}/\text{CE} < 1$ of all
 463 samples measured by Lab-9 could be the result of overestimation of ammonium. Similarly, in
 464 addition to ammonium detection accuracy of >110%, generally lower anion detection
 465 accuracies than cations were reported by Lab-4, which may explain $\text{AE}/\text{CE} < 1$ in all samples
 466 measured by this lab as well. The other three labs (Lab-2, 7 and 8) were found with various
 467 AE/CE ratios with both >1 and <1 values; moderately polluted days were generally observed
 468 with a higher ratio of AE/CE . These results indicate that AE/CE ratios bear large uncertainties
 469 from different labs. Stricter quality control measures should be adopted if applying AE/CE
 470 ratios to evaluate aerosol acidity.

471

472 3.5.2 Ion Balance

473 The calculation of ion balance is an alternative way to evaluate the aerosol acidity (Han et al.,
 474 2016; He et al., 2012). Three methods were listed below for the calculation of ion balance in
 475 this study:

476 Method 1: $IB = 2[\text{SO}_4^{2-}] + [\text{NO}_3^-] - [\text{NH}_4^+]$ (6)

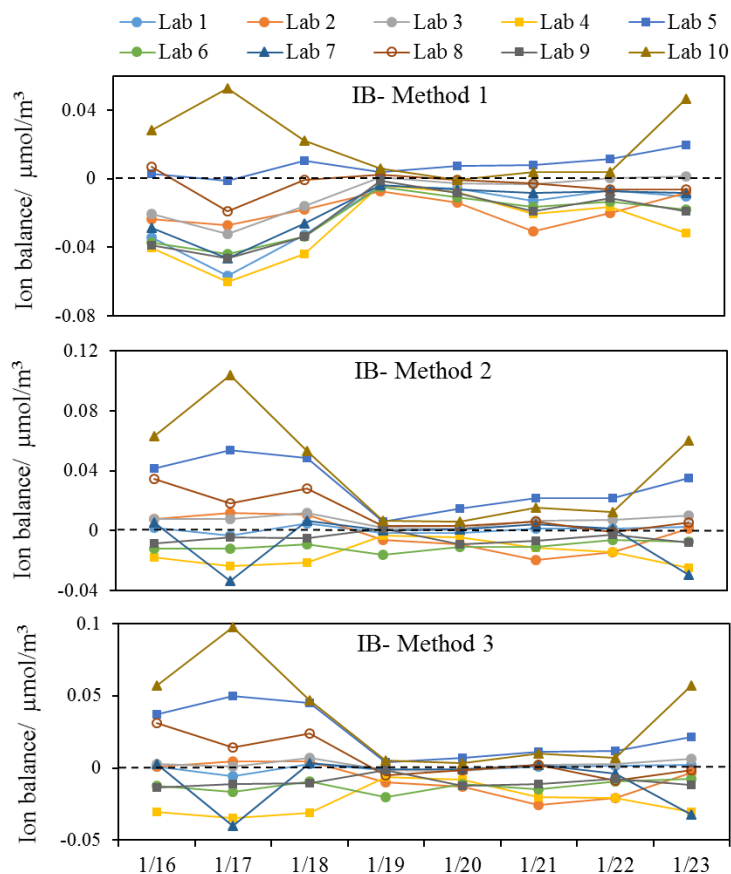
477 Method 2: $IB = 2[\text{SO}_4^{2-}] + [\text{NO}_3^-] + [\text{Cl}^-] - [\text{NH}_4^+] - [\text{Na}^+] - [\text{K}^+]$ (7)

478 Method3: $IB = 2[\text{SO}_4^{2-}] + [\text{NO}_3^-] + [\text{Cl}^-] - [\text{NH}_4^+] - [\text{Na}^+] - [\text{K}^+] - 2[\text{Mg}^{2+}] - 2[\text{Ca}^{2+}]$
 479 (8)

480 In Method 1, only SO_4^{2-} , NO_3^- and NH_4^+ were applied for the calculation (Tian et al., 2017),
 481 assuming that these three ions and H^+ alone control $\text{PM}_{2.5}$ acidity (Ziemba et al., 2007). SO_4^{2-} ,
 482 NO_3^- and NH_4^+ were also used in other studies to assess aerosol acidity. For example, the mole
 483 charge ratio of NH_4^+ to the sum of SO_4^{2-} and NO_3^- was applied to represent aerosol acidity
 484 (Chandra Mouli et al., 2003; Wang et al., 2019). SO_4^{2-} , NO_3^- and NH_4^+ were selected because
 485 they contributed approximately 90% of the total ionic species in fine aerosols and play

486 predominant roles in controlling aerosol acidity (Zhou et al., 2012). Salt ions Na^+ , K^+ and Cl^-
487 were added for the calculation in Method 2. Based on this calculation, Mg^{2+} and Ca^{2+} were
488 added in Method 3 to include the effects of crustal dust on aerosol acidity (Huang et al., 2014).
489 The ion balance of all labs varied applying different methods, especially for the first three
490 heavily polluted days, as shown in Fig. 4. Positive ion balance values indicated a deficiency of
491 cations to neutralize anions, while negative values implied an excess of cations to neutralize
492 anions. Lab-10 showed the highest variation among all labs; when excluding Lab-10, the results
493 of the other 9 labs agreed very well, with most of the values below 0, suggesting sufficient
494 ammonium to neutralize sulfate and nitrate. By applying Method 1, comparable results were
495 found. The average ion balance values in all samples were consistent in Lab-1, 2, 6, 7, 9 (0.02
496 $\mu\text{mol}/\text{m}^3$). When adding more ions in the calculation by adopting Methods 2 and 3, poorer
497 agreement among all labs was exhibited. Therefore, it seems more consistent to indicate the
498 relative ion-balanced aerosol acidity among different samples by Method 1, as SNA were the
499 most abundant ions in atmospheric aerosols and their concentrations measured by different labs
500 showed good agreement (Fig. 1). This method could reduce the large discrepancy of ion
501 balance results calculated by adding other ions from the different labs, as their concentrations
502 varied largely in different labs due to varying detection limits.

503



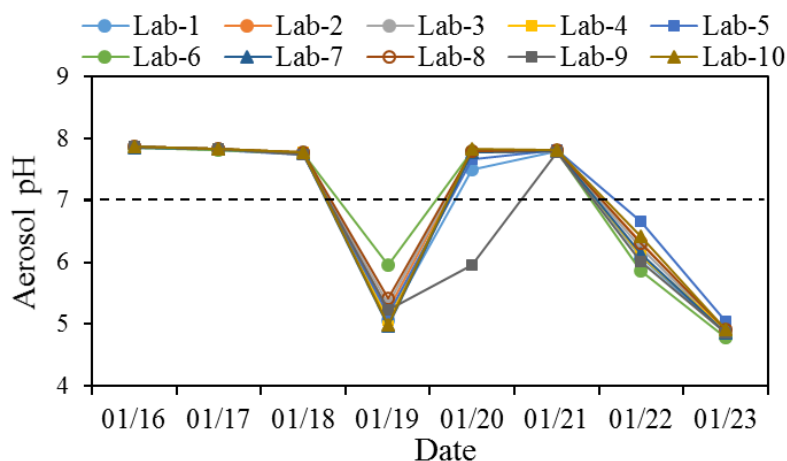
504
 505 **Fig. 4** Ion balance in all labs applying different methods (negative values reflect the excessive cations
 506 to neutralize anions)

507
 508 **3.5.3 Aerosol pH using ISORROPIA-II**

509 A thermodynamic equilibrium model- ISORROPIA-II was applied to estimate the in-situ
 510 aerosol acidity. This was run only in forward mode, as the results from the use of reverse mode
 511 (using only particle phase composition) are reported to be unreliable (Song et al., 2018) . The
 512 only gas phase data were for ammonia, but this introduces little error as concentrations of HNO₃
 513 and HCl are likely to be very low in this high ammonia environment (Song et al., 2018) .

514 The inputs include aerosol-phase Cl⁻, SO₄²⁻, NO₃⁻, Na⁺, NH₄⁺, K⁺, Mg²⁺, Ca²⁺ and gas-phase
 515 NH₃ concentrations. The daily ammonia concentrations during the study period derived from
 516 5-minute data ranged from 13.9±0.6 to 20.1±0.7 ppb (average: 17.2±2.2 ppb). The small
 517 standard deviations of the daily average (< 1 ppb) suggest that the diurnal variation of NH₃ was
 518 not significant. Hence, aerosol pH was only investigated using daily mean NH₃ concentrations.

519 Mean NH_3 concentrations during moderately polluted and non-haze days were 19.6 ± 0.6 and
 520 15.9 ± 1.5 ppb, respectively. Daily temperature ranged between -4.4°C to 4.3°C with an average
 521 of 1.0°C and RH ranged from 13.8% to 40.1% with a mean value of 22.4%. The aerosol pH
 522 was calculated for all samples by the model, as well as aerosol water content (AWC. Table S5),
 523 details of the calculation of pH and AWC can be found elsewhere (Liu et al., 2017b; Masiol et
 524 al., 2020). The calculated aerosol pH results of 10 labs are presented in Fig. 5. The predicted
 525 gas-phase NH_3 by ISORROPIA-II was well correlated with the measured NH_3 with slope of
 526 1.02 and R^2 of 0.95 (Fig. S6), which demonstrated the accuracy of thermodynamic calculations
 527 by the model (Song et al., 2018).



528
 529 **Fig. 5** Aerosol pH estimated by ISORROPIA-II using ions and ammonia in 10 labs from 16th to 23rd
 530 January 2019.

531
 532 The computed aerosol pH during the study period generally exhibited good agreement among
 533 10 labs. Lab-6 was observed with higher pH and lower ion balance than other labs on the 19th,
 534 which could be mainly due to the 2-3 times higher K^+ concentration measured by Lab-6 on that
 535 day (Fig. 1), while other ions measured by this lab were more comparable with other labs. The
 536 aerosol pH on 3 moderately polluted days was above 7, indicating an alkaline nature of aerosols
 537 during these days. This result is consistent with the discussion mentioned above that ion
 538 balance estimated by Method 1 was below 0 as more NH_4^+ neutralizes NO_3^- and SO_4^{2-} . It should

539 be noted that higher pH (>7) of those samples could be due to the lower temperature (-
540 4.4~4.3 °C) during the sampling period (Table S3), in addition to their relatively alkalic nature.
541 The equilibrium of water (H₂O) with OH⁻(aq) + H⁺(aq) is temperature-dependent. For highly
542 dilute aqueous systems, the values of pK_w (= -log₁₀[K_w]; K_w is the temperature-dependent
543 equilibrium constant on molality basis) at 25 °C (13.99) and 0 °C (14.95) can result in
544 corresponding pH values of 6.995 and 7.475, respectively, both of which are considered neutral
545 (Bandura and Lvova, 2006; Pye et al., 2020). In addition, the low RH in these samples (Table
546 S3) may have also contributed to the high pH values we calculated. Different RH values were
547 tested for aerosol pH among 10 labs. The results (Fig. S7) showed that at different RH (40%,
548 50%, 60%, 70%, 80%), the pH values in 10 labs were consistent; and the pH values were mostly
549 lower than 6 in all samples. Hence, higher pH (>7) of some samples could be resulted from the
550 combination of lower temperature, RH, and the nature of the aerosols. Excellent agreement
551 among the 10 labs for the aerosol pH during these moderately polluted days was also found.
552 Non-haze days, especially the least polluted day on 20th, showed higher variation among the
553 different labs. The calculated pH of 9 labs mostly fall on the same side of the neutralization
554 line (pH=7), and only lab-9 on 20th falls onto a different side of the pH=7 line from the other
555 labs. Sensitivity test of Na⁺, K⁺, Mg²⁺ and Ca²⁺ showed that this abnormal pH value was mainly
556 due to the significant higher Na⁺ concentration of Lab-9 on 20th.

557 Our results suggest AE/CE and Ion Balance are flawed representations of particle acidity,
558 which are not recommended for the evaluation of aerosol acidity. This is also consistent with
559 the conclusions from previous studies (Hennigan et al., 2015; Guo et al., 2015; Pye et al., 2020).
560 ISORROPIA-II gives more consistent aerosol pH values among different laboratories. But
561 there are uncertainties within this calculation: 1) RH during some periods in this study was
562 relatively low (around 20%), and as a result, aerosol water content is very low. Under such
563 conditions, ions are mostly existed in solid phase. Hence, pH of aerosols with very low RH

564 may not be reliable; 2) the calculation of AWC only considered for inorganics in this study.
565 Water associated with organics also contribute to AWC. For example, Guo et al. (2015)
566 indicated that it accounts for 29-39% of total PM_{2.5} water in southeastern United States.
567 NH₃ is the main driving factor affecting aerosol pH and leads to the more alkaline nature of
568 aerosols. To investigate the effect of NH₃ concentration on aerosol pH, we conducted a
569 sensitivity test which showed the aerosol pH of samples measured by 10 labs at NH₃ levels of
570 0.5, 1, 2, 5 and 10 ppb (Fig. S8). When the concentration of NH₃ \geq 2 ppb, the aerosol pH
571 estimates of the 10 labs were generally consistent and less affected by the variation of ion
572 concentrations. But there is more variation of aerosol pH in the 10 labs when NH₃ concentration
573 was under 2 ppb. This suggests when NH₃ concentration $<$ 2 ppb, the aerosol pH could be more
574 affected by the variation of ion concentrations. Wang et. al (2020) also reported that the high
575 concentration of total ammonium (gas+aerosol) was likely an important factor causing lower
576 aerosol acidity of fine particles during a severe haze period in Henan province, China. It is also
577 confirmed in another study that ammonia played an important role in influencing aerosol pH
578 during winter haze period in northern China (Song et al., 2018).

579

580 **4. SUMMARY AND RECOMMENDATIONS**

581 Despite use of variable methods and instruments for measuring ion concentrations, data from
582 all the participating labs show a reasonably good agreement in the overall trend for major ions
583 like chloride, sulfate, nitrate, and ammonium. The coefficients of divergence of these ions
584 across 10 labs were lower than 0.2 and the correlation coefficients were higher than 0.8,
585 suggesting a reasonably high reliability of measuring major ions by IC in different labs.
586 However, the inter-lab difference can be as high as 30% if excluding the two extreme values
587 for each day, and reached up to 100% in extreme cases if including all data. Furthermore, ions

588 like F^- , Mg^{2+} , K^+ and Ca^{2+} were observed with large variations in different labs, which may be
589 due to their relatively low concentrations in the samples. Good correlations were found for
590 non-refractory ion species measured by ACSM with those in our study. However, the absolute
591 mass levels were quite different, which may be due to the differences in the performance of the
592 two $PM_{2.5}$ cut-point selectors, the uncertainties in ACSM observations themselves, and
593 negative filter artefacts. Certified reference materials were applied to show the detection
594 accuracy of IC measurement in the 10 laboratories. By comparing the coefficient of variation
595 of samples among 10 labs before and after correction by the detection accuracy of CRM, we
596 emphasize the importance of using certified reference materials for quality control for future
597 ionic species analysis.

598

599 Aerosol acidity was studied through the investigation of ion-balance based acidity and in-situ
600 acidity. Firstly, the ratios of anion equivalent concentrations to cation equivalent concentrations
601 (AE/CE) varied significantly in different labs, which could be attributed to measurement errors,
602 as supported by the different detection accuracies of ions in CRM. Secondly, by calculating the
603 ion balance, Method 1 which only applied SNA for the calculation, was more consistent in
604 most labs. Poor agreement of acidity estimation was observed in all labs when adding other
605 ions like Ca^{2+} and Mg^{2+} . Finally, ISORROPIA-II was applied for estimating in-situ aerosol
606 acidity by calculating aerosol pH in forward (gas+aerosol phases as input) mode. The results
607 showed a similar trend between labs and exhibited a good agreement. This indicates that, if
608 including gaseous pollutant equilibrium in the ISORPIA II model, the estimated aerosol pH is
609 more consistent even if there are relatively large differences in the measured concentrations of
610 ions.

611

612 Based on this analysis and our experience, we recommend that:

- 613 1. Literature aerosol ion data based on online and offline methods should be treated with a
614 degree of uncertainty in mind. The uncertainties are particularly large for minor ions like
615 Ca^{2+} from the aerosol filters-based ion chromatography analysis.
- 616 2. The ion-balance approach is not recommended for estimating aerosol acidity due to its
617 large uncertainty. Instead, in situ aerosol pH may be used to represent acidity, and can be
618 calculated from thermodynamic model considering gas-aerosol equilibrium (e.g., NH_4^+
619 and NH_3). This requires the measurements of aerosol composition as well as NH_3 .
- 620 3. The variation of ion concentrations is expected to strongly affect aerosol acidity estimated
621 by ISORROPIA II when the NH_3 concentration is low (e.g., < 2 ppb in this case).
622 Additionally, the impact of the diurnal variation of NH_3 on aerosol acidity is worthy of
623 investigation, particularly when the NH_3 concentration is low.
- 624 4. Certified reference materials should be used on a regular basis to assess the accuracy and
625 reliability of the measurement method. Calibration standards should be re-prepared and
626 the IC performance should be checked when the detection accuracy is largely deviated
627 from 100% (e.g., $> 110\%$ or $< 90\%$).
- 628 5. The detection accuracy of ammonium varied significantly among 10 labs (88.4-135.0%)
629 with median value close to 100%. Stock NH_4^+ solutions that are used for the preparation
630 of calibration standards should be freshly prepared to ensure good detection accuracy.
- 631 6. Robust quality control processes should be put in place to avoid contamination,
632 particularly for those ions with low concentrations, such as K^+ and Na^+ . For example, water
633 blanks should be run before any standard or sample analyses to ensure no contamination
634 from water blanks or the IC system.

635 7. Some batches of commercial quartz filters may be contaminated with Na^+ and PO_4^{3-} , and
636 thus testing each batch of blank filters is necessary before any field sampling (data not
637 shown here). Filter washing may be needed in some cases.

638 8. Ionic concentration from ACSM observations should be calibrated although the observed
639 trend is robust. Future research should be carried out to compare the offline ASCM and IC
640 using the same filters to clearly identify the discrepancies between the two methods.

641

642 **ACKNOWLEDGEMENTS**

643 This research was funded by the Natural Environment Research Council (Grant Nos.
644 NE/S00579X/1, NE/N007190/1, NE/R005281/1). We would like to thank all researchers for
645 carrying out the technical work and providing the relevant data. We appreciate the support from
646 all participating laboratories.

647

648 *Data availability.* The data in this article are available from the corresponding author upon
649 request.

650

651 *Author contributions.* ZS conceived the study after discovering large inter-lab variability in
652 water-soluble inorganic ions from offline and online methods. JX prepared the paper with the
653 help of ZS, RMH and all co-authors. JX, LW, QZ, CZ, XY, DC, WJL, MW, HT, LiL, ST,
654 WRL, JW, GS, YH, SS, CP, YC, FY, AM, DD, SJS, IA, and JFH conducted the laboratory
655 analysis. SS supported the aerosol pH calculation. CS supported the calculation of coefficient
656 of divergence. YLS, LuL, FZ, KRD, CY, YL, MK provided the ACSM data and YLS supported
657 the interpretation of the ACSM data. BG provided the NH_3 data.

658

659 *Competing interests.* The authors declare that they have no conflict of interest.

660

661 **REFERENCES**

662 Allan, J. D., Delia, A. E., Coe, H., Bower, K. N., Alfarra, M. R., Jimenez, J. L., Middlebrook, A. M.,
663 Drewnick, F., Onasch, T. B., Canagaratna, M. R., Jayne, J. T., and Worsnop, D. R.: A generalised
664 method for the extraction of chemically resolved mass spectra from Aerodyne aerosol mass

665 spectrometer data, *Journal of Aerosol Science*, 35, 909-922,
666 <https://doi.org/10.1016/j.jaerosci.2004.02.007>, 2004.

667 Baltensperger, U., and Hertz, J.: Determination of anions and cations in atmospheric aerosols by single
668 column ion chromatography, *Journal of Chromatography A*, 324, 153-161,
669 [https://doi.org/10.1016/S0021-9673\(01\)81314-5](https://doi.org/10.1016/S0021-9673(01)81314-5), 1985.

670 Bandura, A., and Lvova, S.: The Ionization Constant of Water over Wide Ranges of Temperature and
671 Density, *Journal of Physical and Chemical Reference Data - J PHYS CHEM REF DATA*, 35,
672 10.1063/1.1928231, 2006.

673 Buchberger, W. W.: Detection techniques in ion chromatography of inorganic ions, *TrAC Trends in*
674 *Analytical Chemistry*, 20, 296-303, [https://doi.org/10.1016/S0165-9936\(01\)00068-1](https://doi.org/10.1016/S0165-9936(01)00068-1), 2001.

675 Budisulistiorini, S. H., Canagaratna, M. R., Croteau, P. L., Baumann, K., Edgerton, E. S., Kollman, M.
676 S., Ng, N. L., Verma, V., Shaw, S. L., Knipping, E. M., Worsnop, D. R., Jayne, J. T., Weber, R. J., and
677 Surratt, J. D.: Intercomparison of an Aerosol Chemical Speciation Monitor (ACSM) with ambient fine
678 aerosol measurements in downtown Atlanta, Georgia, *Atmos. Meas. Tech.*, 7, 1929-1941, 10.5194/amt-
679 7-1929-2014, 2014.

680 Chandra Mouli, P., Venkata Mohan, S., and Jayarama Reddy, S.: A study on major inorganic ion
681 composition of atmospheric aerosols at Tirupati, *Journal of Hazardous Materials*, 96, 217-228,
682 [https://doi.org/10.1016/S0304-3894\(02\)00214-5](https://doi.org/10.1016/S0304-3894(02)00214-5), 2003.

683 Chou, C. C. K., Lee, C. T., Yuan, C. S., Hsu, W. C., Lin, C. Y., Hsu, S. C., and Liu, S. C.: Implications
684 of the chemical transformation of Asian outflow aerosols for the long-range transport of inorganic
685 nitrogen species, *Atmospheric Environment*, 42, 7508-7519,
686 <https://doi.org/10.1016/j.atmosenv.2008.05.049>, 2008.

687 Crenn, V., Sciare, J., Croteau, P. L., Verlhac, S., Fröhlich, R., Belis, C. A., Aas, W., Äijälä, M., Alastuey,
688 A., Artiñano, B., Baisnée, D., Bonnaire, N., Bressi, M., Canagaratna, M., Canonaco, F., Carbone, C.,
689 Cavalli, F., Coz, E., Cubison, M. J., Esser-Gietl, J. K., Green, D. C., Gros, V., Heikkinen, L., Herrmann,
690 H., Lunder, C., Minguillón, M. C., Močnik, G., O'Dowd, C. D., Ovadnevaite, J., Petit, J. E., Petralia,
691 E., Poulain, L., Priestman, M., Riffault, V., Ripoll, A., Sarda-Estève, R., Slowik, J. G., Setyan, A.,
692 Wiedensohler, A., Baltensperger, U., Prévôt, A. S. H., Jayne, J. T., and Favez, O.: ACTRIS ACSM
693 intercomparison – Part 1: Reproducibility of concentration and fragment results from 13 individual
694 Quadrupole Aerosol Chemical Speciation Monitors (Q-ACSM) and consistency with co-located
695 instruments, *Atmos. Meas. Tech.*, 8, 5063-5087, 10.5194/amt-8-5063-2015, 2015.

696 Đorđević, D., Mihajlić, A., Relić, D., Ignjatović, L., Huremović, J., Stortini, A. M., and Gambaro,
697 A.: Size-segregated mass concentration and water soluble inorganic ions in an urban aerosol of the
698 Central Balkans (Belgrade), *Atmospheric Environment*, 46, 309-317,
699 <https://doi.org/10.1016/j.atmosenv.2011.09.057>, 2012.

700 Fan, M.-Y., Cao, F., Zhang, Y.-Y., Bao, M.-Y., Liu, X.-Y., Zhang, W.-Q., Gao, S., and Zhang, Y.-L.:
701 Characteristics and Sources of Water Soluble Inorganic Ions in Fine Particulate Matter During Winter
702 in Xuzhou (In Chinese), *Huan jing ke xue= Huanjing kexue*, 38, 4478-4485,
703 10.13227/j.hjkx.201703178, 2017.

704 Fountoukis, C., and Nenes, A.: ISORROPIA II: a computationally efficient thermodynamic equilibrium
705 model for K^+ – Ca^{2+} – Mg^{2+} – NH_4^+ – Na^+ – SO_4^{2-} – NO_3^- – Cl^- – H_2O aerosols, *Atmos. Chem. Phys.*, 7,
706 4639-4659, 10.5194/acp-7-4639-2007, 2007.

707 Ge, B. Z., Xu, X. B., Ma, Z. Q., Pan, X. L., Wang, Z., Lin, W. L., Ouyang, B., Xu, D. H., Lee, J., Zheng,
708 M., Ji, D. S., Sun, Y. L., Dong, H. B., Squires, F. A., Fu, P. Q., and Wang, Z. F.: Role of Ammonia on
709 the Feedback Between AWC and Inorganic Aerosol Formation During Heavy Pollution in the North
710 China Plain, *Earth And Space Science*, 6, 1675-1693, 10.1029/2019ea000799, 2019.

711 Guo, H., Xu, L., Bougiatioti, A., Cerully, K., Capps, S., Hite, J., Carlton, A. M., Lee, S.-H., Bergin, M.,
712 Ng, N., Nenes, A., and Weber, R.: Fine-particle water and pH in the southeastern United States,
713 *ATMOSPHERIC CHEMISTRY AND PHYSICS*, 15, 5211-5228, 10.5194/acp-15-5211-2015, 2015.

714 Guo, H., Sullivan, A. P., Campuzano-Jost, P., Schroder, J. C., Lopez-Hilfiker, F. D., Dibb, J. E., Jimenez,
715 J. L., Thornton, J. A., Brown, S. S., Nenes, A., and Weber, R. J.: Fine particle pH and the partitioning
716 of nitric acid during winter in the northeastern United States, *Journal of Geophysical Research:*
717 *Atmospheres*, 121, 10,355-310,376, 10.1002/2016jd025311, 2016.

718 Guo, Y.-t., Zhang, J., Wang, S.-g., She, F., and Li, X.: Long-term characterization of major water-
719 soluble inorganic ions in PM₁₀ in coastal site on the Japan Sea, *Journal of Atmospheric Chemistry*, 68,
720 299-316, 10.1007/s10874-012-9223-8, 2011.

721 Han, B., Zhang, R., Yang, W., Bai, Z., Ma, Z., and Zhang, W.: Heavy haze episodes in Beijing during
722 January 2013: Inorganic ion chemistry and source analysis using highly time-resolved measurements
723 from an urban site, *Science of the Total Environment*, 544, 319-329, 10.1016/j.scitotenv.2015.10.053,
724 2016.

725 Harrison, R. M., and Pio, C. A.: MAJOR ION COMPOSITION AND CHEMICAL ASSOCIATIONS
726 OF INORGANIC ATMOSPHERIC AEROSOLS, *Environ. Sci. Technol.*, 17, 169-174,
727 10.1021/es00109a009, 1983.

728 He, K., Zhao, Q., Ma, Y., Duan, F., Yang, F., Shi, Z., and Chen, G.: Spatial and seasonal variability of
729 PM_{2.5} acidity at two Chinese megacities: insights into the formation of secondary inorganic aerosols,
730 *Atmos. Chem. Phys.*, 12, 1377-1395, 10.5194/acp-12-1377-2012, 2012.

731 He, Q., Yan, Y., Guo, L., Zhang, Y., Zhang, G., and Wang, X.: Characterization and source analysis of
732 water-soluble inorganic ionic species in PM_{2.5} in Taiyuan city, China, *Atmos. Res.*, 184, 48-55,
733 <https://doi.org/10.1016/j.atmosres.2016.10.008>, 2017.

734 Heckenberg, A. L., and Haddad, P. R.: Determination of inorganic anions at parts per billion levels
735 using single-column ion chromatography without sample preconcentration, *Journal of Chromatography*
736 A, 299, 301-305, [https://doi.org/10.1016/S0021-9673\(01\)97845-8](https://doi.org/10.1016/S0021-9673(01)97845-8), 1984.

737 Hennigan, C. J., Izumi, J., Sullivan, A. P., Weber, R. J., and Nenes, A.: A critical evaluation of proxy
738 methods used to estimate the acidity of atmospheric particles, *Atmos. Chem. Phys.*, 15, 2775-2790,
739 10.5194/acp-15-2775-2015, 2015.

740 Huang, K., Zhuang, G., Wang, Q., Fu, J. S., Lin, Y., Liu, T., Han, L., and Deng, C.: Extreme haze
741 pollution in Beijing during January 2013: chemical characteristics, formation mechanism and role of
742 fog processing, *Atmos. Chem. Phys. Discuss.*, 2014, 7517-7556, 10.5194/acpd-14-7517-2014, 2014.

743 Jia, S., Wang, X., Zhang, Q., Sarkar, S., Wu, L., Huang, M., Zhang, J., and Yang, L.: Technical note:
744 Comparison and interconversion of pH based on different standard states for aerosol acidity
745 characterization, *Atmospheric Chemistry and Physics*, 18, 11125-11133, 10.5194/acp-18-11125-2018,
746 2018.

747 Kamal, A., Syed, J. H., Li, J., Zhang, G., Mahmood, A., and Malik, R. N.: Profile of Atmospheric PAHs
748 in Rawalpindi, Lahore and Gujranwala Districts of Punjab Province (Pakistan), *Aerosol Air Qual. Res.*,
749 16, 1010-1021, 10.4209/aaqr.2015.01.0016, 2016.

750 Karthikeyan, S., and Balasubramanian, R.: Determination of water-soluble inorganic and organic
751 species in atmospheric fine particulate matter, *Microchemical Journal*, 82, 49-55,
752 <https://doi.org/10.1016/j.microc.2005.07.003>, 2006.

753 Kim, C. H., Choi, Y., and Ghim, Y. S.: Characterization of Volatilization of Filter-Sampled PM_{2.5}
754 Semi-Volatile Inorganic Ions Using a Backup Filter and Denuders, *Aerosol Air Qual. Res.*, 15, 814-
755 820, 10.4209/aaqr.2014.09.0213, 2015.

756 Krudysz, M. A., Froines, J. R., Fine, P. M., and Sioutas, C.: Intra-community spatial variation of size-
757 fractionated PM mass, OC, EC, and trace elements in the Long Beach, CA area, *Atmospheric*
758 *Environment*, 42, 5374-5389, <https://doi.org/10.1016/j.atmosenv.2008.02.060>, 2008.

759 Li, L., Yin, Y., Kong, S., Wen, B., Chen, K., Yuan, L., and Li, Q.: Altitudinal effect to the size
760 distribution of water soluble inorganic ions in PM at Huangshan, China, *Atmospheric Environment*, 98,
761 242-252, <https://doi.org/10.1016/j.atmosenv.2014.08.077>, 2014.

762 Li, X., Wang, L., Ji, D., Wen, T., Pan, Y., Sun, Y., and Wang, Y.: Characterization of the size-
763 segregated water-soluble inorganic ions in the Jing-Jin-Ji urban agglomeration: Spatial/temporal
764 variability, size distribution and sources, *Atmospheric Environment*, 77, 250-259,
765 <https://doi.org/10.1016/j.atmosenv.2013.03.042>, 2013.

766 Li, Y., Tao, J., Zhang, L., Jia, X., and Wu, Y.: High Contributions of Secondary Inorganic Aerosols to
767 PM_{2.5} under Polluted Levels at a Regional Station in Northern China, *Int J Environ Res Public Health*,
768 13, 1202, 10.3390/ijerph13121202, 2016.

769 Liu, B., Wu, J., Zhang, J., Wang, L., Yang, J., Liang, D., Dai, Q., Bi, X., Feng, Y., Zhang, Y., and
770 Zhang, Q.: Characterization and source apportionment of PM_{2.5} based on error estimation from EPA
771 PMF 5.0 model at a medium city in China, *Environmental Pollution*, 222, 10-22,
772 <https://doi.org/10.1016/j.envpol.2017.01.005>, 2017a.

773 Liu, M., Song, Y., Zhou, T., Xu, Z., Yan, C., Zheng, M., Wu, Z., Hu, M., Wu, Y., and Zhu, T.: Fine
774 particle pH during severe haze episodes in northern China, *Geophysical Research Letters*, 44, 5213-
775 5221, 10.1002/2017gl073210, 2017b.

776 Liu, Y., Yan, C., Ding, X., Wang, X., Fu, Q., Zhao, Q., Zhang, Y., Duan, Y., Qiu, X., and Zheng, M.:
777 Sources and spatial distribution of particulate polycyclic aromatic hydrocarbons in Shanghai, China,
778 *Science of The Total Environment*, 584, 307-317, <http://dx.doi.org/10.1016/j.scitotenv.2016.12.134>,
779 2017c.

780 Liu, Y., Yan, C., Feng, Z., Zheng, F., Fan, X., Zhang, Y., Li, C., Zhou, Y., Lin, Z., Guo, Y., Zhang, Y.,
781 Ma, L., Zhou, W., Liu, Z., Wei, Z., Dada, L., Dallenbach, K. R., Kontkanen, J., Cai, R., Chan, T., Chu,
782 B., Du, W., Yao, L., Wang, Y., Cai, J., Kangasluoma, J., Kokkonen, T., Kujansuu, J., Rusanen, A.,
783 Deng, C., Fu, Y., Yin, R., Li, X., Lu, Y., Liu, Y., Lian, C., Yang, D., Wang, W., Ge, M., Wang, Y.,
784 Worsnop, D., Junninen, H., He, H., Kerminen, V. M., Zheng, J., Wang, L., Jiang, J., Petäjä, T., Bianchi,
785 F., and Kulmala, M.: Continuous and Comprehensive Atmospheric Observations in Beijing: A Station
786 to Understand the Complex Urban Atmospheric Environment, *Big Earth Data* (under review),
787 10.1080/20964471.2020.1798707, 2020.

788 Masiol, M., Squizzato, S., Formenton, G., Khan, M. B., Hopke, P. K., Nenes, A., Pandis, S. N., Tositti,
789 L., Benetello, F., Visin, F., and Pavoni, B.: Hybrid multiple-site mass closure and source apportionment
790 of PM_{2.5} and aerosol acidity at major cities in the Po Valley, *Science of The Total Environment*, 704,
791 135287, <https://doi.org/10.1016/j.scitotenv.2019.135287>, 2020.

792 Meng, C. C., Wang, L. T., Zhang, F. F., Wei, Z., Ma, S. M., Ma, X., and Yang, J.: Characteristics of
793 concentrations and water-soluble inorganic ions in PM_{2.5} in Handan City, Hebei province, China,
794 *Atmos. Res.*, 171, 133-146, <http://dx.doi.org/10.1016/j.atmosres.2015.12.013>, 2016.

795 Middlebrook, A. M., Bahreini, R., Jimenez, J. L., and Canagaratna, M. R.: Evaluation of Composition-
796 Dependent Collection Efficiencies for the Aerodyne Aerosol Mass Spectrometer using Field Data,
797 *Aerosol Sci. Technol.*, 46, 258-271, 10.1080/02786826.2011.620041, 2012.

798 Mkoma, S. L., Wang, W., and Maenhaut, W.: Seasonal variation of water-soluble inorganic species in
799 the coarse and fine atmospheric aerosols at Dar es Salaam, Tanzania, *Nuclear Instruments and Methods*
800 *in Physics Research Section B: Beam Interactions with Materials and Atoms*, 267, 2897-2902,
801 <https://doi.org/10.1016/j.nimb.2009.06.099>, 2009.

802 Ng, N. L., Herndon, S. C., Trimborn, A., Canagaratna, M. R., Croteau, P. L., Onasch, T. B., Sueper, D.,
803 Worsnop, D. R., Zhang, Q., Sun, Y. L., and Jayne, J. T.: An Aerosol Chemical Speciation Monitor
804 (ACSM) for Routine Monitoring of the Composition and Mass Concentrations of Ambient Aerosol,
805 *Aerosol Sci. Technol.*, 45, 780-794, 10.1080/02786826.2011.560211, 2011.

806 Pathak, R. K., Wu, W. S., and Wang, T.: Summertime PM_{2.5} ionic species in four major cities of China:
807 nitrate formation in an ammonia-deficient atmosphere, *Atmospheric Chemistry and Physics*, 9, 1711-
808 1722, 2009.

809 Pye, H. O. T., Nenes, A., Alexander, B., Ault, A. P., Barth, M. C., Clegg, S. L., Collett Jr, J. L., Fahey,
810 K. M., Hennigan, C. J., Herrmann, H., Kanakidou, M., Kelly, J. T., Ku, I. T., McNeill, V. F., Riemer,
811 N., Schaefer, T., Shi, G., Tilgner, A., Walker, J. T., Wang, T., Weber, R., Xing, J., Zaveri, R. A., and
812 Zuend, A.: The acidity of atmospheric particles and clouds, *Atmos. Chem. Phys.*, 20, 4809-4888,
813 10.5194/acp-20-4809-2020, 2020.

814 Shi, Z., Vu, T., Kotthaus, S., Harrison, R. M., Grimmond, S., Yue, S., Zhu, T., Lee, J., Han, Y.,
815 Demuzere, M., Dunmore, R. E., Ren, L., Liu, D., Wang, Y., Wild, O., Allan, J., Acton, W. J., Barlow,
816 J., Barratt, B., Beddows, D., Bloss, W. J., Calzolari, G., Carruthers, D., Carslaw, D. C., Chan, Q.,
817 Chatzidiakou, L., Chen, Y., Crilley, L., Coe, H., Dai, T., Doherty, R., Duan, F., Fu, P., Ge, B., Ge, M.,
818 Guan, D., Hamilton, J. F., He, K., Heal, M., Heard, D., Hewitt, C. N., Holloway, M., Hu, M., Ji, D.,
819 Jiang, X., Jones, R., Kalberer, M., Kelly, F. J., Kramer, L., Langford, B., Lin, C., Lewis, A. C., Li, J.,
820 Li, W., Liu, H., Liu, J., Loh, M., Lu, K., Lucarelli, F., Mann, G., McFiggans, G., Miller, M. R., Mills,
821 G., Monk, P., Nemitz, E., O'Connor, F., Ouyang, B., Palmer, P. I., Percival, C., Popoola, O., Reeves,
822 C., Rickard, A. R., Shao, L., Shi, G., Spracklen, D., Stevenson, D., Sun, Y., Sun, Z., Tao, S., Tong, S.,
823 Wang, Q., Wang, W., Wang, X., Wang, X., Wang, Z., Wei, L., Whalley, L., Wu, X., Wu, Z., Xie, P.,
824 Yang, F., Zhang, Q., Zhang, Y., Zhang, Y., and Zheng, M.: Introduction to the special issue "In-depth
825 study of air pollution sources and processes within Beijing and its surrounding region (APHH-Beijing)",
826 *Atmos. Chem. Phys.*, 19, 7519-7546, 10.5194/acp-19-7519-2019, 2019.

827 Shon, Z.-H., Kim, K.-H., Song, S.-K., Jung, K., Kim, N.-J., and Lee, J.-B.: Relationship between water-
828 soluble ions in PM_{2.5} and their precursor gases in Seoul megacity, *Atmospheric Environment*, 59, 540-
829 550, <https://doi.org/10.1016/j.atmosenv.2012.04.033>, 2012.

830 Song, S., Gao, M., Xu, W., Shao, J., Shi, G., Wang, S., Wang, Y., Sun, Y., and McElroy, M. B.: Fine-
831 particle pH for Beijing winter haze as inferred from different thermodynamic equilibrium models,
832 *Atmos. Chem. Phys.*, 18, 7423-7438, 10.5194/acp-18-7423-2018, 2018.

833 Song, S., Nenes, A., Gao, M., Zhang, Y., Liu, P., Shao, J., Ye, D., Xu, W., Lei, L., Sun, Y., Liu, B.,
834 Wang, S., and McElroy, M. B.: Thermodynamic Modeling Suggests Declines in Water Uptake and
835 Acidity of Inorganic Aerosols in Beijing Winter Haze Events during 2014/2015–2018/2019,
836 *Environmental Science & Technology Letters*, 6, 752-760, 10.1021/acs.estlett.9b00621, 2019.

837 Sun, J., Zhang, Q., Canagaratna, M. R., Zhang, Y., Ng, N. L., Sun, Y., Jayne, J. T., Zhang, X., Zhang,
838 X., and Worsnop, D. R.: Highly time- and size-resolved characterization of submicron aerosol particles
839 in Beijing using an Aerodyne Aerosol Mass Spectrometer, *Atmospheric Environment*, 44, 131-140,
840 <https://doi.org/10.1016/j.atmosenv.2009.03.020>, 2010.

841 Sun, Y., Wang, Z., Dong, H., Yang, T., Li, J., Pan, X., Chen, P., and Jayne, J. T.: Characterization of
842 summer organic and inorganic aerosols in Beijing, China with an Aerosol Chemical Speciation Monitor,
843 *Atmospheric Environment*, 51, 250-259, <https://doi.org/10.1016/j.atmosenv.2012.01.013>, 2012.

844 Sun, Y., He, Y., Kuang, Y., Xu, W., Song, S., Ma, N., Tao, J., Cheng, P., Wu, C., Su, H., Cheng, Y.,
845 Xie, C., Chen, C., Lei, L., Qiu, Y., Fu, P., Croteau, P., and Worsnop, D. R.: Chemical Differences
846 Between PM₁ and PM_{2.5} in Highly Polluted Environment and Implications in Air Pollution Studies,
847 *Geophysical Research Letters*, 47, e2019GL086288, 10.1029/2019gl086288, 2020.

848 Takami, A., Miyoshi, T., Shimono, A., Kaneyasu, N., Kato, S., Kajii, Y., and Hatakeyama, S.: Transport
849 of anthropogenic aerosols from Asia and subsequent chemical transformation, *Journal of Geophysical*
850 *Research*, 112, 10.1029/2006JD008120, 2007.

851 Tian, M., Wang, H., Chen, Y., Zhang, L., Shi, G., Liu, Y., Yu, J., Zhai, C., Wang, J., and Yang, F.:
852 Highly time-resolved characterization of water-soluble inorganic ions in PM_{2.5} in a humid and acidic
853 mega city in Sichuan Basin, China, *Science of The Total Environment*, 580, 224-234,
854 <https://doi.org/10.1016/j.scitotenv.2016.12.048>, 2017.

855 Wang, S., Yin, S., Zhang, R., Yang, L., Zhao, Q., Zhang, L., Yan, Q., Jiang, N., and Tang, X.: Insight
856 into the formation of secondary inorganic aerosol based on high-time-resolution data during haze
857 episodes and snowfall periods in Zhengzhou, China, *Science of The Total Environment*, 660, 47-56,
858 <https://doi.org/10.1016/j.scitotenv.2018.12.465>, 2019.

859 Wang, S., Wang, L., Li, Y., Wang, C., Wang, W., Yin, S., and Zhang, R.: Effect of ammonia on fine-
860 particle pH in agricultural regions of China: comparison between urban and rural sites, *Atmos. Chem.*
861 *Phys.*, 20, 2719-2734, 10.5194/acp-20-2719-2020, 2020.

862 Wang, Y., Zhang, Q., Jiang, J., Zhou, W., Wang, B., He, K., Duan, F., Zhang, Q., Philip, S., and Xie,
863 Y.: Enhanced sulfate formation during China's severe winter haze episode in Jan 2013 missing from
864 current models, *Journal of Geophysical Research: Atmospheres*, 119, 10.1002/2013JD021426, 2014.

865 Weber, R. J., Guo, H., Russell, A. G., and Nenes, A.: High aerosol acidity despite declining atmospheric
866 sulfate concentrations over the past 15 years, *Nature Geoscience*, 9, 282-285, 10.1038/ngeo2665, 2016.

867 Wongphatarakul, V., Friedlander, S. K., and Pinto, J. P.: A comparative study of PM_{2.5} ambient aerosol
868 chemical databases, *Environmental Science and Technology*, 32, 3926-3934, 10.1021/es9800582, 1998.

869 Xu, Q., Wang, S., Jiang, J., Bhattarai, N., Li, X., Chang, X., Qiu, X., Zheng, M., Hua, Y., and Hao, J.:
870 Nitrate dominates the chemical composition of PM_{2.5} during haze event in Beijing, China, *Science of*
871 *The Total Environment*, 689, 1293-1303, <https://doi.org/10.1016/j.scitotenv.2019.06.294>, 2019a.

872 Xu, W., Liu, X., Liu, L., Dore, A. J., Tang, A., Lu, L., Wu, Q., Zhang, Y., Hao, T., Pan, Y., Chen, J.,
873 and Zhang, F.: Impact of emission controls on air quality in Beijing during APEC 2014: Implications
874 from water-soluble ions and carbonaceous aerosol in PM_{2.5} and their precursors, *Atmospheric*
875 *Environment*, 210, 241-252, <https://doi.org/10.1016/j.atmosenv.2019.04.050>, 2019b.

876 Xue, J., Lau, A. K. H., and Yu, J. Z.: A study of acidity on PM_{2.5} in Hong Kong using online ionic
877 chemical composition measurements, *Atmospheric Environment*, 45, 7081-7088,
878 <https://doi.org/10.1016/j.atmosenv.2011.09.040>, 2011.

879 Yao, X., Yan Ling, T., Fang, M., and Chan, C. K.: Comparison of thermodynamic predictions for in
880 situ pH in PM_{2.5}, *Atmospheric Environment*, 40, 2835-2844,
881 <https://doi.org/10.1016/j.atmosenv.2006.01.006>, 2006.

882 Yu, X.-C., He, K.-B., Yang, F., Yang, F.-M., Duan, F.-K., Zheng, A.-H., and Zhao, C.-Y.: Application
883 of ion chromatography to the determination of water-soluble inorganic and organic ions in atmospheric
884 aerosols, *Journal of environmental sciences (China)*, 16, 813-815, 2004.

885 Yue, F., Xie, Z., Zhang, P., Song, S., He, P., Liu, C., Wang, L., Yu, X., and Kang, H.: The role of sulfate
886 and its corresponding S(IV)+NO₂ formation pathway during the evolution of haze in Beijing, *Science*
887 *of The Total Environment*, 687, 741-751, <https://doi.org/10.1016/j.scitotenv.2019.06.096>, 2019.

888 Zhang, B., Zhou, T., Liu, Y., Yan, C., Li, X., Yu, J., Wang, S., Liu, B., and Zheng, M.: Comparison of
889 water-soluble inorganic ions and trace metals in PM_{2.5} between online and offline measurements in
890 Beijing during winter, *Atmospheric Pollution Research*, 10, 1755-1765,
891 <https://doi.org/10.1016/j.apr.2019.07.007>, 2019.

892 Zhang, J. K., Cheng, M. T., Ji, D. S., Liu, Z. R., Hu, B., Sun, Y., and Wang, Y. S.: Characterization of
893 submicron particles during biomass burning and coal combustion periods in Beijing, China, *Science of*
894 *The Total Environment*, 562, 812-821, <https://doi.org/10.1016/j.scitotenv.2016.04.015>, 2016.

895 Zhang, Q., Jimenez, J. L., Worsnop, D. R., and Canagaratna, M.: A Case Study of Urban Particle
896 Acidity and Its Influence on Secondary Organic Aerosol, *Environ. Sci. Technol.*, 41, 3213-3219,
897 10.1021/es061812j, 2007.

898 Zhao, J., Zhang, F., Xu, Y., and Chen, J.: Characterization of water-soluble inorganic ions in size-
899 segregated aerosols in coastal city, Xiamen, *Atmos. Res.*, 99, 546-562,
900 <http://dx.doi.org/10.1016/j.atmosres.2010.12.017>, 2011.

901 Zhou, Y., Xue, L., Wang, T., Gao, X., Wang, Z., Wang, X., Zhang, J., Zhang, Q., and Wang, W.:
902 Characterization of aerosol acidity at a high mountain site in central eastern China, *Atmospheric*
903 *Environment*, 51, 11-20, <https://doi.org/10.1016/j.atmosenv.2012.01.061>, 2012.

904 Ziemba, L. D., Fischer, E., Griffin, R. J., and Talbot, R. W.: Aerosol acidity in rural New England:
905 Temporal trends and source region analysis, *Journal of Geophysical Research: Atmospheres*, 112,
906 10.1029/2006jd007605, 2007.

907 Zou, J., Liu, Z., Hu, B., Huang, X., Wen, T., Ji, D., Liu, J., Yang, Y., Yao, Q., and Wang, Y.: Aerosol
908 chemical compositions in the North China Plain and the impact on the visibility in Beijing and Tianjin,
909 *Atmos. Res.*, 201, 235-246, <https://doi.org/10.1016/j.atmosres.2017.09.014>, 2018.

910